Dear Editor,

Please find below the detailed answer to both referees major and minor comments. These corrections have been implemented in the text, several supplementary figures have been added (width estimate validation, correlation of the storm parameters, correlation between landsliding and climate normalized rainfall , …), and several main text figures have been updated.

We almost never opposed the referees comments, and performed some re-analyses as they suggested. Two modifications arise from these (re)-analyses :
1/ The correlation between storm duration and landslide position and slope faded, and is now only evocated. The result that rainfall induced landslides do not strongly oversample steep slopes remain and is characterized more robustly.
2/ A correlation between landslide scar areas and storm metrics was found and it is now presented and discussed.

The rest of our results and discussion presented before has not significantly changed and we hope is now clearer.

Review of Marc et al. "Towards a global database of rainfall-induced landslide inventories: first insights from past and new events" by David Milledge.
Major Comments
This is a well executed study with novel and interesting findings. I have three general comments and a large number of minor comments but neither the major nor minor comments reflect a fundamental problem in the research in my view.

I am not convinced that it is essential (or helpful) to present your inventories as the only inventories that are suitable for this type of analysis (as you seem to do on P2-3). Instead you could simply say they are one set of inventories and they demonstrate the power of this type of approach. I am not convinced of the need for landslides beneath an entire storm footprint to be mapped and am sceptical that entire storm footprints can be convincingly defined so I'm not convinced by your critique of studies that analyse far smaller study areas (other than on sample size grounds).

The methodology description could be more consistent between inventories. Similar information is reported for each case but the style of the reporting differs and some key information reported in some cases is not present in others (e.g. image source, image resolution, acquisition date).
>> To clarify the methodology, we first include a short paragraph about the general methodology. Then we have made sure to include all imagery type, dates and spatial resolutions for each event.
The style remains somewhat different given the variations in methodology/specific knowledge for each case.

I am not convinced that your focus on 'comprehensive' inventories is necessary nor that examination of total landslide numbers, volumes or areas are particularly meaningful in relation to rainfall triggered landslide inventories (though I think the findings on landslide density and slope are extremely interesting and thought provoking). This focus might reflect a desire for comparability to co-seismic landslides but I think the two triggers are importantly different. For example, it is extremely difficult to define the spatial and temporal limits on a single storm. In addition I find the results relating to total numbers, volumes and areas less convincing because they are predicted from a small number of point rainfall records. A clearer explanation of why 'comprehensive' inventories and total statistics are important would be a valuable addition to the paper.

Minor Comments
P1L4: Associated to: How do you know that these events are associated to one another.
>>We replaced "associated to" with "coincident with" : all the inventory presented can be dated within a few hours or days leaving a single rain-storm as a trigger. Of course this does not exhaust the question of antecedent "preparatory" conditions.

P2
L8: deterministic approaches inapplicable: I think this statement is a little strong. Is it really fair to

say that they are inapplicable given their data requirements.
>> Original meaning was that in those places without enough data (i.e. most places) the deterministic approach is inapplicable. We rephrase to:
"In most places, such level of detailed information is currently unavailable, rendering deterministic approaches hardly applicable."
L30: comprehensive: this term needs defining.
>> We mean that all landslides detectable above the spatial resolution limit were mapped, and that we could observe the landslide density fading away in all direction, indicating the limits of the footprint of the high intensity part of the storm.
We will specify this two criteria in the main text. We added in the introduction :
"By comprehensive inventories we mean that all landslides larger than a given size were mapped, and that the extent of the imagery allowed to observe the landslide density fading away in all direction, tracking the reduction of the forcing intensity of the triggering event, whether shaking or rainfall."

L34: Why is it insufficient? I think you need to demonstrate this. Is this a sample size argument? Some things won't be possible to calculate but others will. What can you and can't you do with a subset inventory and how big does the subset need to be?. Is it ever possible to capture the full inventory for a storm? How do you define its bounds?
>> Following the referee advice we focus this point on sample size and biased sampling. We also refer to fragmentary inventories rather than catchment scale :
We rephrased to : "Although relatively rare, some case studies based on fragmentary event inentories exist (and are briefly reviewed in the next section) but they may contain too few landslides for statistical analyses or may be biased to specific locations (along roads or near settlements, within weak lithological units, downslope, etc), thus complicating the deconvolution of forcing versus site influences."

We address the question of storm definition and bound elsewhere (cf P3 L7).

P3
L4: landslide scale: I am not clear what this means. Could you define it?
>>We meant studies that focus on small samples of individual landslides, and landslide scale was ambiguous there. We now rephrase it:
"... we consider that neither studies based on small sample of individual landslide or on global-scale analysis will be able to constrain effectively Eq 1..."

L7: comprehensive mapping: where do you start and finish. Your definition of a storm is very important here and I don't see it at the moment. For example shouldn't the Morakot mapping extend to the Phillipenes and China on this basis?
>> The pragmatic answer is that the landslide response in Philippines and China was negligible compared to the one in Taiwan (We doubled check that quickly by looking at Landsat images where no hyperpycnal flows or alluviations in stream exiting hilly areas are visible, contrarily to Taiwan where these processes are very clear). Same is true if we look at landsliding in the rest of Japan hit by Typhoon Talas progressing Northward after hitting the Kii peninsula. This may be in part due to topographic difference, but I think this is also due to the fact enormous amount of rainfall was poured on this topography, probably largely because of orographic effects (cf Chien and Kuo 2009, Taniguchi et al., 2009). Thus preceding rainfall on less high topography (e.g. in the Philippines) probably received much less rainfall, and the following rainfall over China (or Japan for Talas) was also likely less heavy because little or no recharge over the ocean was possible and a significant fraction of the typhoon moisture was used up.

More generally a proper "object" definition is hardly achievable in Meteorology as we deal with a continuous fluid which suffers perturbations with scales interactions and as meteorological events are not independent from each other. Therefore not all atmospheric specialists agree on the definition and limit of a single 'storm' . Ideally, future studies could categorize storms according to some space-time filtering and analyze their relations with landslides for each storm category. Currently, our database in not sufficient for this.

Also our ability to measure the characteristic of a 'storm' or rainfall event depends on its spatio-temporal extension (sampling a large and long lasting storm is more robust than sampling a very localized event)

We added in the discussion, P19 L30: "In any case, several caveat should be taken with the preliminary scaling between total storm rainfall and total landsliding. First the definition and limit of a single "storm" is not generally

agreed in the meteorological community, because the atmospheric fluids suffers perturbations with scale interactions, and therefore with events not independent from each other. Ideally, future studies could categorize storms according to some space-time filtering and analyze the scaling with total landsliding for each storm category. Currently, our data base is not sufficient for this yet."

L14: adequately: how do you quantify adequate representation, what would inadequate representation look like and how do you know whether a representation is adequate?
>> We meant an adequate representation of the landslide population, i.e., one population that represent (and thus average) the different processes that lead to landsliding. This means a sufficient number, with comprehensive representation of the different landslide size above a threshold etc. This point is developed in comments P4L4.

We replaced "representing adequately" by a neutral term : "containing".

L30: this gets at a difficult issue, what do you include as a landslide? I think you need a clear definition that can be applied across all inventories and I don't see one at present. Divergence from the definition in different inventories will introduce bias to your results.
>> We tried to avoid mapping (or remove in the already mapped inventories (J11, TW9) deposition and erosion in the fluvial system, broadly defined as the areas with permanent flows, visible in the high resolution image. This meant that debris flow on hillslope would be mapped but not its prolongation within the fluvial system. We considered bank collapses as a disturbance that would be localized, usually not symmetric and not necessary linked to a landslide/debris flow on the hillslopes. Clearly we may miss some bank collapse, and where to put the limit between a debris flow on a hillslope and its continuation on the fluvial channel is difficult and somewhat subjective. However, if amalgamation is avoided, the width estimate (and thus scar area and volume) will be relatively insensitive to these issues, that mainly affect the total runout and aspect ratio.
We added at the start of the section 2.2:
"Here we consider landslides as a rapid downslope transport of material, disturbing vegetation outside of the fluvial domain, which we define by visible water flow in the imagery. We also consider individual landslides with a single source or scar areas to avoid amalgamation, and split polygons when necessary. Although the transition between hillslopes and channel may be blurry and in part subjective, the width estimation (cf. 2.4) will mitigate variations of the transport length, as long as large alluviated, or flooded areas are not mapped as landslide deposits. "

P4L4: whether or not the statistical properties of a subset are representative: you need to demonstrate that they are not representative for your argument here to hold and it is not obvious that this is the case. They might not be representative because of the sample size but why should you need the all landslides triggered by a particular storm, it seems reasonable to assume that one catchment is independent of another for these processes and on these timescales.
>> We mostly agree with the referee. We will develop the description along these lines:

1/ number is always important, in absolute terms because below 50-100 landslides the reliability of any statistical processing is uncertain but also in relative terms, because a statistical study based on 500 landslides out of a storm that caused ~5000 take the risk to have biased interpretation if the (potential) specificity of the subset population are not noticed and understood (e.g., mostly large landslide ?, mostly landslide near river ? Mostly landslide in a given lithology ? Etc etc).

2/ If enough landslides are mapped within an AOI (e.g., >50-100 in total, > 75% of landslides above the spatial resolution limit, leading to a reasonable frequency-size distribution) the inventory above the AOI is likely to be statistically usable and representative of the various processes and conditions affecting the process in the AOI. Then a partial inventory will indeed allow to study any local parameter and their variations within the AOI : e.g. landslide density, landslide size distribution, relations to slope etc.

3/ However, a comprehensive inventory may have the additional advantage to gather enough landslide across different areas (in terms of lithology, relief etc) potentially allowing to establish a hierarchy in controlling parameters and also allowing to study an averaged landslide response less likely to be dominated by specific site effects. comprehensive inventories are the only ones allowing to study the variations of total landsliding.

We removed this sentence and the next and replaced it by :

"These inventories could not constrain the total landslide response to a storm, but may allow to constrain

relationships between landslide properties and local rainfall, provided that enough landslides have been mapped for statistical analysis (e.g., >50-100) and without any systematic sampling bias. However, a detailed assessment of these datasets properties and of their relation to rainfall is out of the scope of this study although it would probably complement interestingly our work in the future."

We also rephrased a conclusion sentence: "… show the value of mapping systematically a large sample of the landslides that can be related to a single storm ..."

P5
L15-19: why take this approach rather than breaking up the multi-headed polygons manually?
--> In this study, the multiheaded polygons have often equivalent width and it is likely that they contribute equally to the overall runout and deposit. Breaking up the different head to reflect equivalent contribution would have been impractical.
We rephrased : "The surface of the source areas were often of similar width, suggesting equivalent contribution from each source to the transport and deposit areas, and rendering a manual splitting impractical. "

L6-17: this methods description is difficult to follow. Image acquisition dates and image resolution information is missing in some cases. It would also be useful to give some indication of the performance of the automated classification with respect to manually mapped landslides.
>> We specified the dates and resolution of the Geoeye and Landsat 7 images.
"30m Landsat 7 images from February 2011 "

"very high resolution Geoeye-1 image (2/0.5 m resolution in multispectral/panchromatic) from the 26th of May 2010 and the 20th of January 2011."

P7
L1: there is quite a long window between pre and post event imagery in some cases. How confident can you be that another storm did not trigger some of the landslides? What evidence do you have that this is the case?
>> Although this may have not been clear enough, instantaneous imagery was available in M02, C99, B11 (90%), J11 and most of C15 (~85%). The 2 years were probably referring to C15 where we have few cloud less images on the AOI, but the event is also dated by a HR images in Google Earth from 31st of May 2015 (cdf P7 L12 comment below). The other intervals are much shorter and without other storms of the same magnitude.

USGS reports with VHR image also shows ~50-75% of landslides in C15. B08 (90%zone)
M02 and C99 were verified fresh on the field. For the other case we rely on pre-event imagery :
Pre-event Google Earth imagery in B11 in most place.
15 July for J11.
For TW 2009, we have a clear Landsat image on 24 of June (day 175, for some reason it was noted 255 in TableSuppl 1) and then the Formosat images were taken on the week after Morakot. Thus although some landslide may have happen during smaller scale storms before the start of August it would be negligible compared to the number of slides triggered by Morakot.
For TW8 we have 32 days between the mapping images. In the south the intermediate image is foggy but allows to see intact vegetation on the hillslope. Only the Northernmost landslide cluster, near Sun Moon Lake is fully masked by clouds but some Aster images allow to confirm that most of what is mapped was not present before mid July. Also, the rainfall from the 15th to 20th of July was much stronger than anything in the previous 3 weeks.

L2: mapped automatically: I think you need to include a methods description for this automatic mapping and some information on how the quality of this mapping was evaluated.
>> We had made some confusion here, as the landslides were not automatically mapped there. Only the mapping quality was problematic as many slides were connected through channel deposits and alluviation. We rephrased : "For subsets of the inventory, especially to the East of the main divide, landslides were significantly amalgamated and bundled with river channel alluviation. We thus manually split the polygons and removed the channel areas."

L4: fluvial system: How do you define the fluvial system and how did you identify it for the study

area?
>>The fluvial system was broadly defined as the areas with permanent flows, visible in the high resolution image. As we do not perform any analysis on the relation between the hydrographic network and landslide this approach is just aiming at making sure landslides are limited to hillslopes. Therefore we added in our definition of landslide : "the fluvial domain, which we define by visible water flow in the imagery." (cf comment P3 L30)

L5: to map at least the largest: I don't understand what this means, were there some areas of your study area that you did not have high resolution imagery for? If so what fraction of the study area was this and what impact does this have on the inventory as a whole?
--> Yes in Taiwan 2008, and 2009, or in small sub-area of Brazil 2008, or Japan 2011, we could not get high resolution image close enough in time to confidently validate our low resolution mapping done (in TW8 and B11) or the emergency mapping of NILIM done with airphotos in Japan.
In figure 1, the yellow boxes shows footprint of VHR images (Google Earth in most cases) sufficiently close in time. In TW8 this is the whole inventory. IN Taiwan 2009, the pan-sharpened Formosat imagery has 2m spatial resolution, and only the cloud covered areas (~5%) where mapped with low spatial resolution Landsat images. In B08 and B11 <10%, in J11 ~15%.

We rephrased : "In a few areas with clouds (~300 km² in total or <5% of the AOI) in the post-event mosaic, we mapped with Landsat 5 images (from 24th of June and 12th of September 2009), even if the spatial resolution limit may have censored the smallest landslides."

We also specified the area covered by HR imagery :
In Japan : "With Google Earth we could validate NILIM on about 85\% of the AOI and we added ..."
In Brasil 2008: "Therefore we used extensively high-resolution imagery available in Google Earth (over >90\% of the AOI) acquired in May-June 2009"

In Brasil 2011: "we mapped landslides directly from Google Earth (available over >90\% of the AOI)"

The impact of low spatial resolution is mainly on the landslide number, but not likely significant on the total area and volume or even landslide density, as discussed in the results section.

L12: Specific dates are missing for the Landsat images. This is a 2 year window, which seems a very long time. How confident can you be in assigning landslides to a single event within that window and what is the basis for this confidence? This is particularly important given your earlier critique of other inventories
>> We forgot to indicate it here but Google Earth contains a mostly cloud free images covering most of the dataset dated from 31st May 2015. The scar look very fresh in this image and corresponds well with the "new" scars observed by comparing the 2016-2014 images.
We specify now:
"Landslide mapping was carried out by comparing a (10 m) Sentinel 2 image from the 21st of July 2016 and a pan-sharpened (15 m) Landsat 8 image from the 19th of July and the 26th December of 2014. These images were selected for their absence of clouds, good conditions of light and similarity. High spatial resolution imagery from Google Earth, dated from the 31st of May 2015 shows fresh scars consistent with our mapping over most of the area (Fig 1), and we assumed that the remaining landslides (<15% of the inventory) were also triggered by the same rainfall event. "

L20-21: maximal forcing: this doesn't seem to be consistent with your argument for the importance of complete landslide footprints. You are comparing the forcing at a single location within the footprint to the properties of the entire footprint.
>> Well the maximum forcing is taken as a "storm magnitude", and it is compared to total landsliding and peak landslide density close of this maxima l forcing, so we think the approach is reasonable.
We think that the issue of the referee is that in the introduction we push for "comprehensive landslide inventory" and later do not make fully use of it. This for 2 reasons: 1/ We have access to extensive rainfall data constraining the spatial pattern of rainfall for only a few cases, and the analysis of the spatial pattern is beyond the scope of this study and left for a future study (Marc et al., in Prep).

2/ Generally a comparison of storm magnitude with total landsliding requires an accurate order of magnitude of the total landsliding. We think that the fact that storm magnitude correlates well with total landsliding suggest some internal correlation between the peak total rainfall, and the mean rainfall and its variability within the storm footprint. Still we acknowledge that such correlation may not hold for all type of rainfall events: In our database, small events are likely brief convective thunderstorm (C99,C15), while large ones are typhoons (M02,TW8,TW9, J11), so very large singular system that are loaded during their displacement over ocean, and unloaded on landfall, even more importantly when hitting high relief. The cases of B08 and B11 is more complex as it more likely results from interactions between oceanic moisture and specific meteorologic conditions on land.

We specify now : "… but rather maximal forcing, which may be taken as a storm magnitude, ..."
and at the start of the next paragraph:
"A more detailed analysis of the spatio-temporal pattern of the rainfall and of its relations to the spatial pattern of landsliding is highly desirable, but challenging and is left for a future study."

In the discussion, after mentionning the diffulty to define a storm we added :
"Second, linking total rainfall in a limited area and the total landsliding within the storm footprint implicitly suggests that storm rainfall is somewhat structured with some internal correlations between peak rainfall, storm size, and the spatial pattern of rainfall intensity within the storm. This seems to be the case for large tropical storms (Jiang_ et al.,2008), but should be explored for a broader range of storm types. Orographic effects (e.g., Houze, 2012; Taniguchi et al., 2013), focussing high intensity rainfall on topographic barriers, may also enhance such correlation between local total rainfall, and the broader pattern of rainfall and landsliding."

L30: landslide densities: calculated over what window size, I think that this choice will be critically important. On a small window density will have multiple local peaks.
--> We forgot to specify it in the main text (but it is on the caption of Fig S2) : 0.05x0.05° so approximately 25km². It is true that multiple peak can appear at smaller resolution, however considering only the magnitude of the peak landslide density, the trend observed in Fig X was not changing for cells of 0.02° to 0.1°.

L33: why not use 3 gauges for Colorado? Where were the next nearest gauges and why were they discounted?
>> The second closest gauge (LB) is ~2 km North and 3km West from the Grizzly Peak station, at the limit of the airphoto area in Fig 2, and it recorded 13mm on the 28th of July (43 for Grizzly Peak). The third stations (JG) is a couple of kilometer south of the study area and recorded 20 mm. Radar data shown by Godt and Coe (2007) indicates the afternoon rainfall reached 25-35mm/hr along the peaks eastward and northeastward of the GP stations while it was only ~6mm/hr near LB or at the southern edge of the study area (presumably to JG).
We will add in the main text:
"For the Colorado 1999 storm, radar data indicate very localized high intensity precipitation located on the peaks were debris flow occurred (Godt and Coe 2007) and suggest that the single closest gage is more representative than averaging with the other nearby ones."

P8L11: continuous period: I'm not totally clear what this means, does it mean that if there was no rain in a 3 hour period then that is the end / start of the storm? Was the same duration criteria applied to all records?
>> Yes we meant that the conditions I3<3 mm/hr was the start/end of the storm. However, this can be directly apply only in TW8,TW9, J11, C99, M02 we do not have this information for B08 B11 and the threshold for the satellite data in C15 may be different, as mentioned in the text.
Thus we just added "continuous period when rainfall was sustained (I3>3mm.hr-1)"

P9
L5: how, and where, did you measure landslide width?
--> The width was initially measured by GIS on a limited number (~50) of randomly selected slides in Colombia and Japan. To make this point more robust we proceeded as follow:
We rephrased in the revised manuscript (also updating our assumption about the aspect ratio):
"To validate this geometric method to retrieve landslide width we measured systematically the width of 418 randomly selected landslides across all range of polygon area and aspect ratio, belonging to four inventories: J11, TW8, B11, and C15. For each polygon, we focused on the upper part of the landslide only, the likely scar, and averaged 4 width (i.e., length perpendicular to flow) measurements made in arcGIS. The width estimated based on P

and A are within 30% and 50% of the measured width for 72% and 92% of the polygons, respectively (Fig Suppl 5).We do not observed a trend in bias with area nor aspect ratio, except perhaps for the automatically mapped landslide in B11, where high aspect ratio correlates with underestimated width. Thus, for correctly mapped polygons we can use P and A to derive W and a proxy of landslide scar area, A_s ~ 1.5 W^2. We assume landslide scars have an aspect ratio of 1.5, as it was found to be the mean aspect ratio found across a range of landslide size within a global database of 277 measured landslide geometries (Domej et al., 2017). Even if this equivalent scar area may not exactly correspond to the real landslide scar, it effectively removes the contribution of the landslide runout to the landslide size and allows to compare different size distributions while reducing the impact of variable runout distances."

This should also clarify that we compute W based on Perimeter and Area.

L6: I think you could state this more simply by saying that you assume that scars have equal length and width. This is the same assumption used by Pelletier et al., 1997.
--> This would have been an option. However, we became aware of a study presented at EGU general assembly of 2018, where the aspect ratio of a number of landslide scar has been analyzed. Domej et al., 2017, reported that in average the length-width ratio remained close of 1.5 for all landslide size. So we follow them and assume that 1.5 represent a good average of the length width ratio of landslide scar.

Cf Previous Comment P9 L5

P10
L23: isolated remote landslides: how were these defined?
>> We refer to single or small group of landslides without other landslides in the surrounding, usually on the fringes of the landslide population.

We specify now in the text : "(i.e., single or small cluster of landslides without other landslides within 5-10 km)"

L24: to what extent is the landslide distribution area constrained by your study area (i.e. the extent of available images). Taking this to an extreme did Typhoon Morakot trigger landslides in China or the Phillipenes and should these also be included? This again reflects something that I think you need to discuss somewhere, the differences between rain storms and earthquakes as triggers: where are they similar enough to borrow frameworks from one another and where do they differ?

>> **Well it is clear that, contrarily to earthquake that have a well delimited source (across the fault), the rainfall forcing is moving together with the storm and can travel over significant areas.**

This aspect has been discussed in comments P3 L7 and P7 L20-21

P11
L3: typically have power law: they have typically been fit with these distributions but do we know that they typically follow that distribution or do we fit power laws tailed distributions without testing alternatives (e.g. log-normal).
>> Some studies have tested various distributions option and find Pareto distribution (Stark and Hovius 2001, 1 dataset) or Inverse Gamma distributions to fit best (Malamud 2004, 3 datasets) but this debate is out of the scope of our work.
We rephrase with : "have typically been fit by power-law tailed distributions."

L19: must also: must is a strong statement, could it alternatively be due to different mapping criteria?
-> We changed "physical parameters must influence" to "However, mechanical parameters are also expected to influence the roll-over position (Stark and Guzzetti, 2009, Frattini and Crosta 2013), as suggested by the fact that MI2, mapped with 1m resolution ... "
as these studies have propose physical models (of slope stability or probabilistic rupture propagation) where both the roll-over and power-law decay are influenced by mechanical properties.

L24: peculiar distributions: are these distributions peculiar if you are seeking power laws but not if other alternatives are considered? Have you tried a log-normal distribution? Negative curvature of the tail in log-log space sometimes indicates better fits for log-normal distributions?

>> The question is difficult to solve and not so important for our studies: Fitting log-normal distribution by MLE we obtain better agreement for some distributions and worst for others (comparing the Kolmogorov-Smirnov Test statistic and Anderson Darling test statistic obtained for log-normal or IGD fit obtained by MLE).

In other work the Inverse Gamma distributions has been found to provide the best fit to 3 large landslide catalogue (Malamud 2004). Further some work on the theoretical emergence of landslide size distribution also predict power-law decaying tail (Stark and Guzzetti 2009), with a tail related to the mechanical properties of the medium, implying the debate may not only be a question of goodness of fit, especially given that some datasets may be affected by artifacts.

Although we can mention these facts, solving such a debate is clearly out of the scope of our work. Thus we simply added the following statement : "In these two cases, for whole landslide area or landslide scar only, we note that a MLE fit of a lognormal distribution agrees better to the data (based on the result of both the Kolmogorov-Smirnov and the Anderson-Darling test). In other inventories a lognormal fit is equivalent or worse than an IGD, but the functional form of landslide size distribution and its implication are beyond the scope of this study. "

L26: Why use a least square fit to represent the power law tail? The problems associated with using least squares fits to binned data rather than an MLE have been widely discussed (e.g. White et al., 2008; Clauset et al., 2009) and Clauset et al. (2009) provide appropriate tools to fit only the power law tail using an MLE.

--> We removed the least square fit and only present the IGD and LogNormal MLE estimates. We updated the text consequently (cf previous comment).

Updating all exponents we found that although whole landslide area is not correlated to rainfall a correlation exist for landslide scar area, with larger rainfall causing more large landslides, thus we updated the result section and added a main text figure. :

"The decay exponents of the distribution of landslide whole area do not correlate significantly with any storm metrics (Intensity, duration or total rainfall) ($|R|<0.1$). However, after runout normalization, the decay exponent of landslide scar area correlate with all metrics, although with significant scatter ($R^2 \sim 0.5$ Fig \ref{area}, Suppl. 7). The two largest storms (J11 and TW9) have the lowest exponents ($\alpha+1\sim1.8$), and thus a large proportion of very large landslides, while the two smallest storms (C15 and C99) have a small proportion of large landslides and large exponents ($\alpha+1\sim2.7$). However, intermediate cases are very scattered, as B11 and TW8 have similar total rainfall, peak intensity and duration but very different distribution with $\alpha+1=1.9$ and with $\alpha+1=1.9$, respectively."

And in section 3.2.3:

" The decay exponents of the distribution of landslide whole area do not correlate significantly with any storm metrics (Intensity, duration or total rainfall) (|R|<0.1). However, after runout normalization, the decay exponent of landslide scar area correlate with all metrics, although with significant scatter (R^2 ~ 0.5 Fig 4, 7). The two largest storms (J11 and TW9) have the lowest exponents (alpha+1 ~1.8), and thus a large proportion of very large landslides, while the two smallest storms (C15 and C99) have a small proportion of large landslides and large exponents (alpha+1 ~2.7). However, intermediate cases are very scattered, as B11 and TW8 have similar total rainfall, peak intensity and duration but very different distribution with alpha+1 =1.9 and with alpha+1 =2.6 , respectively. Still, randomly removing one event (i.e., jackknife sampling) we obtained R^2 between 0.4 and 0.7, with a similar mean R^2 about 0.5. "

The discussion, conclusion and abstract have also been updated to mention this positive influence (even if partial) on the size distribution.

L29: aspect ratio below 2: why below 2? What are the specifics of the equation? I had understood it

to be A=w^2, which would give an aspect ratio of 1.
--> This is now updated based on Domej 2017 (Cf comments above). This is a reduction to an aspect ratio of 1.5. We corrected that in the main text.

P12
L4-8: Why is this censoring of low slopes necessary? I am not clear on what you are trying to achieve by removing them?
>> The valley floors have a slope distribution mainly between 0 and 10°, likely strongly affected by DEM uncertainties. Still in some zone, most of the affected area may be dominated by floodplain and hillslopes may be a fraction of the AOI. But landslide scar never occur in the valley plain and should be compared to hillslopes rather than to these floodplains. However, a slope criteria cannot be used (as there may be slope <5° within the hillslope domain (ridges, shoulder). Instead we use an elevation criteria for Micronesian Island, and we masked out the flat areas in B08. We added: "allowing to obtain a hillslope distribution as an approximate Gaussian, with a mode significantly beyond our threshold of 5°."

L8-10: generating a histogram then smoothing it seems an unusual approach to this problem, results will likely be sensitive to both the smoothing window and smoothing function. Given the theoretical basis for Kernel density estimation (e.g. Cox, 2007), why not use this approach?
>> We thank the referee for his suggestion. We reanalyze the slope data with a kernel density smoothing, using a normal kernel and optimized bandwidth. We rephrased :
"To focus on the scar area of each landslide polygon, we extracted only the slopes for the highest elevation pixels representing a surface of 1.5*W.^2. Then, we computed the probability density function for the landslide affected area and whole topography (hereafter the "landslide" and "topographic" distribution) with a normal-kernel smoothing with an optimized bandwidth, as implemented in Matlab."

P13
L5: initiation point: I don't think you have previously defined this or explained how these points are identified.
--> We added in the data section on past inventories: "Initiation point were assumed to be the highest point upslope of each mapped landslides. In 57 out of 328 polygons multiple initiation points (2 to >15) were mapped for multi-headed polygons (Godt and Coe 2007)."

L11: focussing on scar areas seems sensible but this particular approach seems strange and the choice of modal topographic slope somewhat arbitrary, could you provide a more robust explanation for this choice? Alternatively couldn't you have used your previously defined scar area (w^2) to identify scars as the highest w^2 area of each polygon? This would be consistent with your previous definition and would avoid introducing an arbitrary slope threshold which could bias the results.
--> We followed the referee suggestion and we extracted the most elevated fraction of each polygon corresponding to an area of ~1.5*W². See P12 L8-10 comment.

Doing this, all curves have slightly shifted to higher slopes. But the main results that most rainfall events do not tend to trigger landslides on very steep slopes remain. Most events do not over-sample more than 1.5-2 times the topographic distribution, much less than the ChiChi example or the C99 rainfall event.

L14: Could you use line thickness to indicate the slope beyond which small numbers of cells in the value range preclude interpretation of the line? It would be useful for the reader to know where that point is for each dataset. Also could you colour the lines in Fig 5 by storm duration? This might make it easier to pick out the behaviour you are identifying in the text and to make a connection between 5A and 5B.
>> We now computed the prediction interval for a random draw out of the topographic distribution, and only interpret the landslide probability that significantly differs from it.

We added : "An important issue is to determine whether the landslide probability can be considered a random drawing from slopes of the topography or not. Given that landsliding affect less than 10\% of the landscape, the sampling of the topography by landslides can be approximated by a Bernoulli sampling. In this case, the central limit theorem gives the 95\% prediction interval as P_T +/- 1.96 \sqrt(P_T(1-P_T)/N), with N the number of independent

draws, here taken as the number of landslide scars. The convergence of N draws to P_T within the prediction interval is only valid if N>30, N P_T>5 and $N (1-P_T)>5$, implying that only very large samples can be interpreted towards the extremity of the topographic slope distribution, where P_T is small."

And in the figure caption: "The ratios are estimated with the PDF averaged within 3° bins. Solid circles and dots represent ratios where the landslide probability is beyond or within, respectively, the 95\% prediction interval of the topography distribution. Crosses indicate bins where data are insufficient for the validity of the Central Limit Theorem required to estimate prediction interval."

Importantly, the case of C15 with the smallest landslide number (N=171) does not allow to distinguish confidently topographic and landslide distribution at high slopes. Thus only C99 significantly oversample topographic slopes. We updated the results and the discussion ass follows:

Results : in 3.1.2: "For all events we observe that P_L is significantly different from a random drawing of the topography with oversampling of the slopes beyond S_M and undersampling below it (Fig 4B). However, we note that for most events, the undersampling and oversampling is smaller than a factor of 2. Some cases (C15, J11 and TW8) have stronger oversampling (>4) for $S-S_M >25$ but they may not be representative ratios given the limited number of landslides and of slopes thus steep (i.e. $N P_T <5$). The scars of C99 clearly departs from this behavior, with undersampling and oversampling of a factor of 10 and 6 at $S_M \pm 10°$, respectively. B08 has also strong undersampling below S_M but has a landslide distribution that rapidly converges to the topographic one at high slopes. "

in 3.1.3: "We have observed that almost all of our eight events behave similarly with respect to the distribution of topographic slopes, not suggesting strong link with the individual storms properties. The C99 events has a different behavior and was indeed the shortest storm with the smallest total, but it was also the only cases occurring in high elevation terrain, with sparse vegetation. C15, the second shortest and smallest storm event may also have strong oversampling about 20° beyond S_M but the limited number of landslides does not allow to confirm the significance of this oversampling."

We also updated accordingly the last paragraph of the discussion:

This framework might explain the preferential location on steep slopes observed for the very short duration C99 and possibly C15 (Fig \ref{slope}). However, the statistics of C15 are weak and C99 strong oversampling may relate mainly to specific mass movement triggered by surface runoff such as rilling and firehose (cf., Godt andt Coe, 2007). These processes also require high intensity, short duration events, but also low surficial infiltration rate leading to overland flow able to mobilize relatively loose surface materials.

"For other events, we analyzed the slope-gradient vs drainage area relationship for topography and landslide subset and did not find clear over-sampling of high-drainage and gentle gradient areas in the landslide distribution. It is well possible that a 30m DEM is not able to resolve accurately the fine-scale pattern of slope and drainage on the hillsides, where landslides occur, but it may also suggest that the upslope drainage area is not the main explanation. For example, the subsurface drainage efficiency may also increase with slope gradient, thus making very steep areas less likely to develop large pore pressure and possibly explaining the preferential landsliding of slopes just above the modal slopes for almost all events, indepedent of rainfall properties. Hydro-mechanical modeling at the catchment scale [e.g.,](von Ruette et al., 2013), applied on several of our dataset may be the only way to test between these different hypothesis."

P17L9: Total storm rainfall: These results are extremely interesting. They suggest that absolute rainfall properties are good predictors for landslide properties. In the rainfall threshold literature there has been debate over whether absolute rainfall properties are driving failure or whether it is the degree of deviation from normal conditions (e.g. expressed as percentiles). It might be useful if you could reflect on this in relation to your findings. Would a plot of rainfall percentiles for these storms look very similar to the plot of absolutes that we see here?

>> Rainfall percentiles are too difficult to establish for our database and within the scope of this review. However we added discussion on the relevance of normalized rainfall index, showed that storm total normalized by mean monthly rainfall correlates relatively well with landsliding.

We also underline in the mean text that although total rainfall may be a good predictor of the relative amount of landsliding between different storm (as shown in Fig 6 and 7) the control on landsliding must be more compliacted as in the surrounding area similar rainfall occur without triggering landslides (Taiwan, Japan), or in the same

season similar total rainfall did not trigger landslide (in Colorado), so either antecedent rainfall or some constraints on intensity will be needed to generalize /strengthen the results we found.

We added in the main text : "However, we can envision that landscapes may rapidly reach an equilibrium in which all slopes unstable under rainfall conditions frequently occurring would have been removed. In this framework, the rainfall amount relative to the local climate would be more relevant than absolute rainfall, requiring an analysis in terms of deviation from the mean rainfall or in terms of rainfall percentiles (e.g., Guzzetti 2007). Although we could not define rainfall percentiles in each area, we note that normalizing R_t by the mean monthly rainfall relevant for each storm, we still find a decent correlation with the peak landslide density, implying climate normalized rainfall variable may be driving landsliding (Fig Suppl. Z). We also note that even if R_t allows to distinguish the magnitude of different landslide events additional constraints may be needeed to distinguish landslide from non-landslide event, given that for several cases we observe little or no landsliding in surrounding areas or during previous storms with similar rainfall amount. "

P18L17: we have no clear physical explanation: isn't this something that either extreme rainfall community or the hurricane community have thought about? It would be useful to point readers to key reference from that literature here even if you don't strongly back one particular explanation.
>> We replaced the original sentence ("We have no clear physical explanation of why this could be the case, and cannot exclude that it is a coincidence allowed by our small number of events.") by the following discussion :

"For tropical storms and hurricanes (5 out 9 cases in Fig 6D) a number of studies (cf., Jiang, et al., 2008 and ref therein), found that the maximum onland storm total rainfall (i.e, R_t for us) correlated well (R>0.7) with a rainfall potential defined as the product of storm diameter, storm mean rainfall rate within this diameter over storm velocity, each terms measured 1-3 days before landfall. It was also generally observed that rainfall intensity is higher closer of the storm core, thus potentially tightening the link between R_t and a given storm radius with intense rainfall and high landslide probability. These observations would imply linear proportionality between R_t and A_d and could be consistent with the observed power-law trend (1.5) (Fig 6), especially if some further links between R_t and mean storm intensity or velocity exists. Potential links between R_t and A_d for smaller scale storms (C99,C15, B08 and B11) are harder to interpret, we cannot exclude that it is a coincidence allowed by our small number of events."

Jiang, H., Halverson, J. B., Simpson, J. and Zipser, E. J.: Hurricane "Rainfall Potential" Derived from Satellite Observations Aids Overland Rainfall Prediction, J. Appl. Meteor. Climatol., 47(4), 944–959, doi:10.1175/2007JAMC1619.1, 2008.

References
Clauset, A., Shalizi, C.R. and Newman, M.E., 2009. Power-law distributions in empirical data. SIAM review, 51(4), pp.661-703.
Cox, N.J., 2007. Kernel estimation as a basic tool for geomorphological data analysis. Earth surface processes and landforms, 32(12), pp.1902-1912.
White, E.P., Enquist, B.J. and Green, J.L., 2008. On estimating the exponent of power-law frequency distributions. Ecology, 89(4), pp.905-912.

Typographic errors and wording suggestions
P1
L10: storm -> storms
ok
L15: rainfalls -> rainfall
ok

P2
L7: At this day -> at present
Removed

L22: allow to make -> allow

ok

L23: region -> regions
ok
L23: (large slope -> (hillslope

L26: These progresses have - > this progress has#
ok
P3
L7: delete: , and thus
ok

L15: inventory > inventories
ok
L17: it isn't clear what you mean here, perhaps add: size (total area), geometry (length, width and depth) etc.
ok
L25 were > was
ok

P4
L15: N-s should be Ns
ok
L34: avoid > avoids
ok

P5
L2: twice more: or twice the number (i.e. 3n or 2n)?
>> corrected to "twice the number" (2n).
L31: you use a variety of date formats which is a little confusing.

L34: dates are needed for the FORMOSAT-2 image acquisition.
>> They are given following MM/DD format. All are in 2009 as we specify now.

P6: letters missing from Fig 1. Colours of landslides are very difficult to distinguish.
>> Ok We are using BW hillshade to enhance landslide visibility.
P7
L23-27: I don't think this is relevant here, I suggest moving to the discussion.
>> We removed it. This already discussed somewhat in P17L24-26
L30: average record properties: it isn't immediately clear what you mean here.
>> We mean we take the average of the 3 gage records. Removing the word record may make it clearer: In each case we took the three closest gauges within 5 to 15km from the areas with the highest landslide densities (in 0.05 by 0.05° window) (Fig Suppl. 2) and computed their average properties

L33: closest of > closest to
ok

P8
Table 1 caption: Reference are as follow > References are as follows
ok
L10: other > over
ok
L20: is > are
ok
P9
L1: polygons > polygon
ok
L3: allows > allows us

ok
P10
L25: the built > the
ok
L26: 0.2 and > 0.2 to
ok
P11
L10: with important total precipitation: this doesn't seem the right set of words
>> With large total precipitation
P13
L13: artifact due to > artefacts of
ok

P16
L4: S??: figure details missing.
Ok

P18
L23: prime > primary
ok
P21L5: storm tends > storms tend
ok

Anonymous Referee #2

Received and published: 16 May 2018

General Comments

In this manuscript, the authors Marc et al. seek to understand what governs the spatial and geometric characteristics of rainfall-induced landslides that result from single storm events. Toward that end, they compile a database of landslide inventories from single storm events spanning the past twenty years. The database is well considered and thorough, and the strengths and limitations of each are discussed (e.g., availability of local rain gauge data, etc.). With this dataset, the authors then compare landslide spatial characteristics (number of landslides, area affected by landslides, landslide density) and geometric characteristics (landslide total area, landslide scar area) with precipitation characteristics (rainfall duration, storm intensity, total rainfall). In this analysis, the authors make a number of interesting findings. For example, they find that the longer-duration storms result in an increasing number of lower-gradient landslides. Additionally, they show that while landslide volume and spatial density vary as a nonlinear function of storm total rainfall, other landslide parameters do not appear to depend on storm characteristics such as rainfall intensity. From this analysis the authors conclude that their global inventory of single-event rainfall-induced landslides can be queried to answer fundamental questions about the spatiotemporal evolution of landslides in response to hydrologic forcing.
Understanding at a broad scale how a landscape may respond to a given storm event is fundamentally useful for both geomorphic and hazard assessment applications, and this topic should appeal to the readership of ESurf. The rigorous dataset compilation by the authors provides a sound basis to start better quantifying these relationships, and the statistical methods applied to the dataset are well founded and consistent with those used by the community and should be readily reproducible by other researchers

(assuming the database will be available online). The observed correlations between storm magnitude and landslide area draw an interesting parallel to empirical studies of coseismic landslides (e.g., Keefer, 1994), and the data support the authors' conclusions both that rainfall magnitude (expressed as total storm rainfall) is a good indicator of landslide hazard potential and that the increase in lower-sloped landslides occurring over longer duration storms may reflect timescales for water to infiltrate lower portions of the landscape. Although the idea of rainfall-induced landslides occurring in lowersloping sections of a hillslope is well established (e.g., Reid and Iverson, 1992; Densmore and Hovius, 2000), this work shows that the prominence of this effect potentially depends on the storm magnitude and duration.
In terms of the general aspects of the manuscript presentation and layout, I find that the paper needs some fine-tuning and clarification, but overall it is close to being a finished product. The abstract provides a clear summary of the work, and the overall structure and segmentation of the manuscript is easy to follow. The title largely makes sense, although I find the last section stating "first insights from past and new events" confusing since all datasets are within the past twenty years and the youngest event occurred in 2015, and I'm not sure what that phrase adds to the description of the research. There are a number of places where language needs to be altered slightly, and I've tried to provide examples below in the technical comments section of the review. Mathematical formulae appear to be largely correct, but abbreviations for the landslide inventories (although intuitive) are not defined before they are used. Additionally, I found that Figure 2 should be modified, as it is very difficult to see the pink landslide polygons draped over the red and green topography. I imagine this would be especially difficult for people who are red-green colorblind. The supplementary material complements the manuscript well, and I have a few comments regarding supplementary figures below. Although I have a few additional concerns related to content and clarification, overall I think this paper will make an interesting contribution to Esurf..

>> We thank the reviewer for its interest in our study and findings.

From these general comments we retain :
1/ A clarification of Figure 1 (not 2) showing the landslide inventories with a black and white hillshaded

2/ Some edits of the title : Following The discussion with Referee 1 we propose the following new title:
" Initial insights from a global database of rainfall-induced landslide inventories: the weak influence of slope and strong influence of total storm rainfall"

3/ Check that all landslide variables are defined in the text, and improve and correct texts, following both Referees technical comments.

1st Paragraph: I'm not sure I agree with the statement that the goal of constraining quantitative relationships between landslide occurrence and rainfall is out of reach. The authors cite examples of this in the same paragraph. I do agree that there is certainly room for improvement in his area, which I think is the implied sentiment here.
>> Out of reach was maybe exaggerated. We replaced "out of reach" by "difficult".

Equation 1. I appreciate that the authors' goal here is to try to bridge the gap between purely deterministic models and purely statistical models, but I think that there needs to be a little more clarity. At the end of Paragraph 1, for example, you state that certain parameters such as permeability and cohesion that are required for deterministic approaches make a landscape-scale approach in data-poor regions inapplicable, yet you specifically include those parameters in your idealized semi-deterministic Equation 1. Why then is a deterministic approach not appropriate? I think that a bit more discussion might clarify these discrepancies.
>> Deterministic approach will require a fine scale representation of porosity and its variability at a fine scale: more or less the one of the landslides, so at 10-100m. In a semi-deterministic approach we may need only a constrain on the mean porosity (and perhaps some other aspect of its distribution like its variance or skewness) within a whole catchment or 10x10km catchment. Obtaining such information remains a challenge but may be more tractable, and may be correlated to other large scale observable (From hydrological behavior to soil maps ?).

We added "Note that variables in such equation may be statistical description at the catchment or landscape scale (being a simple mean or other moments of the distribution), and thus may not describe the finescale variability required by mechanistic models."

Page 4
Lines 31-34: I'm confused by this sentence. When specifically are data from 2010-2012 used? When May-June 2009 data are not available for a specific location in the landslide-affected area?
>> Exactly. We will clarify this, but in most places in this case imagery just after the event is available in Google Earth.
We rephrased : "... imagery available in Google Earth acquired in May-June 2009 in most areas, and in 2010-2012 elsewhere, where scars were still visible"

Section 2.2 overall.
I'm also confused with the general methodology here. You map landslides on 30 m Landsat imagery, as well as on higher resolution imagery within Google Earth, but only in areas where a negative change in NDVI was observed at the 30 m scale. You then say that field mapping in the area reports twice as many landslides than was observed via remote sensing, but that the missing landslides must be smaller than #1 m resolution. Could the missing landslides not just be in areas that didn't result in a negative NDVI shift in the landsat imagery? For example, a small translation or slump in a forested area may not affect a 30 m pixel.
>> This is true, it would however be relatively small landslide: indeed landslide much smaller than a landsat pixel (e-g, ~5x5m rather than 30x30m) that looked fresh were almost systematically causing reduction of NDVI in one or 2 pixel, although the NDVI reduction was smaller than for large landslides.
So the Landsat NDVI is very sensitive to sub-pixel size landsliding, but the Google Earth imagery is essential to only map landslides and not many other anthropogenic/biological processes changing the NDVI.

We rephrased: "To avoid mapping post-event landslides, we mapped only the ones corresponding to vegetation radiometric index (e.g. NDVI) reduction for the pair of Landsat 5 images, present even for sub-pixel landslides (e.g., 10x5m)."

Page 11
Lines 23-27: In your discussion of peculiar landslide frequency distributions, you focus on deviations from the (perhaps) expected Inverse-Gamma distributions at the large end of the distributions. What about deviations on the smaller end? For example, in the Total Area distributions, TW9, B11, C99, and J11 deviation from the maximum likelihood estimations pretty substantially for small landslide areas. Converting total landslides area to landslide scar area (As), the TW9 distribution especially deviates quite far from the expected P values. Is there a known reason for these deviations? I am far from an expert on landslide frequency distributions, but it seems worth discussing since it is quite apparent on Figure 3!
>> In agreement with Referee 1 we will also add a few line about the quality of IGD vs Lognormal. However, this will remain superficial given deciding on the functional form of size distribution is clearly out of the scope of our paper.

For the deviation in small landslide size, they are difficult to interpret because after the roll-over, censoring issues and difficulty to distinguish multiple adjacent landslides are likely important even with high resolution imagery.

No changes made.

Figure 3: Similarly, I don't believe it is mentioned why the authors choose to break up their landslide populations into two groups. Is this just to more easily visualize? Or is it based on the quality of datasets?
>> Indeed the split is just for visualization. We will specify it in the caption:

“To improve visualization we split the 8 inventories in two groups. ”

Page 15
Lines 11-12: Is there a plot that shows the relationship described on these lines? I couldn’t find one. Maybe it would be worth including these in the supplemental material.
>> Ok we will add such a figure in the supplement.

Page 16
Lines 8-9: Very cool.
>> Thank you, this is indeed exciting.

Page 18
Lines 12-15: If there is a continuous forcing of heavy rainfall over an extended period of time, it is not clear to me why a monsoon would not fit in with the scaling relationships derived in this paper. Would that not be an end-member condition for considering the role of water infiltration in setting the spatial distribution of landslides on lower slopes? If not, then why not? I imagine other people not as familiar with monsoon dynamics like myself might ask the same question.
>> The reviewer is certainly right about the slope distribution, but not for the scaling between total rainfall and landsliding. To clarify the point we added:
Page 18 L20: "Indeed, in a long period with fluctuating rainfall such as the monsoon, drainage and storage of water will certainly not be negligible and the derivation of a soil water content proxy will be necessary (cf., Gabet et al., 2004) ."

Given the scaling between storm duration and slope sampling is not as clear as before after the revision of the method we do not comment further on it.

Page 19
Line 14: Does the proportion of flat ground affect the slide aspect ratios as well, since the flat ground may provide more accommodation space for runout?
>> Locally maybe, but here these sentence really relate to the availability of topography within the footprint of the storm event dominated by the amount of submerged area or flat plains not by the width of valleys that may affect landslide runout.

No changes made.

Line 22: This sentence cannot be true, as Figs. 6 and 7b all show a relationship between storm metrics on landslide scar areas. Do you mean other storm metrics outside of storm total rainfall?
>> Here, the reviewer confuses the total area (counting only scar or whole landslide) shown in Fig 6A, 6B and 7, and the individual scar area distribution shown in Figure 3.
To avoid such confusion for other readers we rephrase to :
"We do not find a clear influence of storm metrics on the probability distribution of individual landslide scar areas or landslide runout (Fig 3)."

Page 20
Line 20: This is almost certainly true, especially for the smaller-area landslides that depend on local slope smaller than what a 30 m pixel can resolve.
>> We also think that. Thus an analysis with a high resolution DEM may be needed.

Technical Corrections
Page 1

Line 3: “..we have very few datasets of rainfall-induced landslides.” I think this should be clarified that this is the case only for single-event inventories.
>> rephrased to : mostly because we have very few inventories of rainfall-induced landslides caused by single storms.

Line 6: should be “orders of magnitude”
>>ok
Line 8: “The non-linear scaling with total rainfall.” Two notes: 1) “nonlinear” is one word;
2) the variable that is being scaled with total rainfall should be specified.
>>The nonlinear scaling of landslide density with total rainfall
Line 11: “contrarily” should be “contrary”
>>ok
Line 18: “..itself expected to increase with global change.” I find this sentence slightly confusing. Consider replacing “itself” with “which are”
>>Ok
Page 2
Line 26: should be “This progress has been possible”
>>Ok
Page 3
Line 5: Should be “is needed”
>>Ok
Line 7: Sentence fragment “: : :affected by the storm, and thus . “
>> This sentence has been replaced following Ref 1 : “Although relatively rare, some case studies based on fragmentary event inentories exist (and are briefly reviewed in the next section) but they may contain too few landslides for statistical analysis or may be biased to specific locations (along roads or near settlements, within weak lithological units, downslope, etc), thus complicating the deconvolution of forcing and site influences."

Lines 13-18: Nice overview!
>>Ok
Line 20: should be “datasets” (plural)
>>Ok
Line 25: should be “The rainfall was”
>>Ok
Line 30: “details” should be singular
>>Ok
Sections 2.1 and 2.2 – Introduce acronyms (e.g., B08) as you introduce each dataset.
>>Ok

Page 4
Line 29: “(30m)” I think a space usually goes between the value and the units, e.g., “30 m”. This should be done consistently throughout the manuscript.
Figure 1. It would be very helpful to make the landslide inventory polygons and rain gauge stations contrast more with the background. The topography could easily be represented as a hillshade since the absolute elevations are not the focus of the figure.
Also, the panels are not labeled with letters as described in the caption.
In the caption, “Landslides inventory” should be “Landslide inventories”
>> We have homogenized space for units. We use now black and white hillshaded DEM for Fig 1 and included the letters to label the panels.

Page 7
Line 2: “sub-parts” could be “subsets” perhaps?
>>ok

Page 8
Lines 2-3: The values and units appear italicized in one instance and standard font in the other. Should be consistently reported.
>> All units will be in standard font.

Lines 5-6: I think “rain gauge” is the correct spelling
>>Ok

Lines 13-14: Is the correlation between D and Rt and I3 and Rt shown anywhere? May be good for the Supplemental.

>> We added a supplementary figure for that.

Line 21: Probably good to put a reference here where the increased runout for larger volume slides is discussed (e.g., Legros, 2002).
>> Here our point is not on the fact that large volume may have more runout, but rather that landslide with long runout may not obey the empirical relations V ~ aA^g (Larsen et al., 2010).

Page 10
Line 8: "However, for subset with less" should be "However, for subsets with fewer"
>>Ok
Line 10: "uncertainties" should be "uncertainty"
>>Ok

Page 11
Line 1: Sentence could be simplified here, e.g., "Landslide inventories typically exhibit heavy-tailed, power law frequency size distributions"
>>This was modified following the other referee suggestion: Frequency size distribution of landslide inventories have typically been fit by power-law tailed distributions,...

Line 14: "Fitted" should be "Fit"
>>Ok

Page 12
Line 9: the term "a slope gradient units" is confusing.
>> Rephrased to : **This ratio represents the tendency of landslide occurrence on a given slope to be more or less frequent than the expected occurrence of this given slope in the landscape.**

Line 10: before the word "oversampling", "and" should be "an"
>>Ok
Line 30: "create" should be "creates"
>>Ok
Line 34: Should there be a figure reference here?
>>Ok Fig 6.

Page 13
Line 7: Should reference Fig. 5d here.
>>Ok

Figure 5: In Figure 5b, you could define the axis value more clearly on the axis itself. "Landslide sampling on steep slopes" does paint a clear image of what the axis value represents.
>> Figure 5B has been removed.

Page 14
Unit labels are italicized and inconsistent with other unit labels throughout the text.

Page 16
Line 4: remove "S??"
>>Refers to Fig Suppl 4. Corrected.
Page 17
Line 3: Could reference Fig 5b specifically.
>>Ok

References
Densmore, A. L. & Hovius, N. Topographic fingerprints of bedrock landslides. Geology 28, 371–374 (2000). Keefer, D. K. The importance of earthquake-induced landslides to long-term slope erosion and slope-failure hazards in seismically active regions. Geomorphology 10, 265–284 (1994). Legros, F. The mobility of long-runout landslides.

Eng. Geol. 63, 301–331 (2002). Reid, M. E. & Iverson, R. M. Gravity-Driven Groundwater Flow and Slope Failure Potential. Water Resour. Res. 28, 939–950 (1992).

~~Towards~~ Initial insights from a global database of rainfall-induced landslide inventories: ~~first insights from past~~ the weak influence of slope and ~~new events~~strong influence of total storm rainfall

Odin Marc[1], André Stumpf[1], Jean-Philippe Malet[1], Marielle Gosset[2], Taro Uchida[3], and Shou-Hao Chiang[4]

[1]École et Observatoire des Sciences de la Terre – Institut de Physique du Globe de Strasbourg, Centre National de la Recherche Scientifique UMR 7516, University of Strasbourg, 67084 Strasbourg Cedex, France
[2]Géoscience Environnement Toulouse,Toulouse,France
[3]National Institute for Land and Infrastructure Management, Research Center for Disaster Risk Management, Tsukuba, Japan
[4]Center for Space and Remote Sensing Research, National Central University, Taoyuan City 32001, Taiwan

Correspondence: Odin Marc (odin.marc@unistra.fr)

Abstract. Rainfall-induced landslides are a common and significant source of damage and fatality worldwide. Still, we have very little understanding of the quantity and properties of landsliding that can be expected for a given storm and a given landscape, mostly because we have very few ~~datasets~~ inventories of rainfall-induced landslides caused by single storms. Here we present six new comprehensive landslide ~~inventories associated to~~ event inventories coincident with well identified rainfall events. Combining these datasets, with two previously published datasets, we study their statistical properties and their relations to topographic slope distribution and storm properties. Landslide metrics (such as total landsliding, peak landslide density or landslide distribution area) vary across 2 to 3 ~~order of magnitudes~~ orders of magnitude but strongly correlate with the storm total rainfall, varying over almost 2 orders of magnitude for these events. ~~Correlation increases when we apply~~ Applying a normalization on the landslide runout distances ~~. The non-linear scaling~~ increases these correlations and also reveals a positive influence of total rainfall on the proportion of large landslides. The nonlinear scaling of landslide density with total rainfall should be further constrained with additional cases and incorporation of landscape properties such as regolith depth, typical strength or permeability estimates. We also observe that, ~~for storm with longer duration,~~ rainfall-induced landslides do not occur preferentially on the steepest slopes of the landscape, ~~contrarily~~ contrary to observations from earthquake-induced landslides~~, suggesting~~ . This may due to the preferential failures of larger drainage area patches with intermediate slopes or to the lower pore-water pressure accumulation in fast draining steep slopes. The database could be used for further comparison with spatially resolved rainfall estimates and with empirical or mechanistic landslide event modeling.

1 Introduction

Landslides associated with heavy ~~rainfalls~~ rainfall cause significant economic losses and may injure several thousand people a year worldwide (Petley, 2012). In addition, the frequency of landsliding increases with that of extreme rainfall events (Kirschbaum et al., 2012), ~~itself~~ which are expected to increase with global change (Gariano and Guzzetti, 2016). Landslides are also recognized as a major geomorphic agent contributing to erosion and sediment yield in mountainous terrain (Hovius et al., 1997; Blodgett and Isacks, 2007). Yet, constraining quantitatively relationships between landslides and rainfall metrics remains ~~out of reach~~difficult.

We have some theoretical understanding of how rainfall, through water infiltration in the ground, can increase ~~pore water~~ pore-water pressures and trigger failures (Van Asch et al., 1999; Iverson, 2000). Therefore a variety of mechanistic models have been developed, usually by coupling a shallow hydrological model to a slope failure criterium ~~(e.g., Montgomery and Dietrich, 1994; Baum~~ However, such deterministic approaches require not only appropriate physical laws, but also an accurate and fine-scale quantification of many input parameters (topography, cohesion, permeability, rainfall pattern)(Uchida et al., 2011). ~~At this day~~In most places, such level of detailed information is ~~unavailable in most places and render deterministic approaches inapplicable~~currently unavailable, rendering deterministic approaches hardly applicable.

Data-driven studies have mostly focused on using precise information on individual landslide location and timing to decipher thresholds, typically based on preceding rainfall intensity and duration, at which landslide would initiate (Caine, 1980; Guzzetti et al., 2008, and references therein). Although useful for hazard and early-warning purposes (e.g., Keefer et al., 1987), such approaches completely ignore the number, size and other properties of landslides that can be triggered by a rainfall event, while these properties are useful, if not required for most natural hazard or geophysical applications. In order to understand the importance of rainfall on erosion rates or to anticipate landslide hazard associated with emerging cyclones and heavy rainstorms, it is highly desirable to quantitatively relate the properties of a landslide event $\mathbf{L}$ (total area, volume, size distribution) to the combination of site susceptibility, $\mathbf{s}$, and rainfall forcing, $\mathbf{f}$, properties, or equivalently to develop scaling relations of the form of:

$$\mathbf{L} = g(\mathbf{s}(slope,\ soil\ thickness,\ strength,\ permeability, ...), \mathbf{f}(total\ rainfall,\ intensity,\ antecedent\ rainfall, ...)) \quad (1)$$

Note that variables in such equation may be a statistical description at the catchment or landscape scale (being a simple mean or other moments of the distribution), and thus may not describe the finescale variability required by mechanistic models. Although being simplified versions of mechanistic models, such scaling laws can be useful to describe average properties of the phenomena, here a population of landslides associated with a constrained trigger. The value of statistical or semi-deterministic approaches is that they are able to predict accurately global properties, while circumventing the difficulties of predicting specific local properties of individual landslides. Indeed, such scaling laws would allow ~~to make~~ prediction in data scarce ~~region~~ regions and possibly at various scales (~~large slope~~ hillslope scale, catchment scale, region scale, etc). This approach has driven important progress for both the understanding and hazard management of earthquake-induced landslides, thanks to the introduction of purely empirical, physically inspired or mixed functional relations in the form of Eq. 1 (e.g., Jibson et al., 2000; Meunier et al., 2007, 2013; Nowicki et al., 2014; Marc et al., 2016, 2017). ~~These progresses have~~ This progress

has been possible thanks to, first detailed investigation of individual case studies with comprehensive landslide ~~inventories (e.g., Jibson et al., 1994; Liao and Lee, 2000; Yagi et al., 2009)~~ event inventories (e.g., Harp and Jibson, 1996; Liao and Lee, 2000; Yagi e
next through their combined analysis as aggregated databases (Marc et al., 2016, 2017; Tanyaş et al., 2017). By comprehensive event-inventories we mean that all landslides larger than a given size were mapped, and that the spatial extent of the imagery allowed to observe the landslide density fading away in all direction, tracking the reduction of the forcing intensity of the triggering event, whether shaking or rainfall.

In contrast, very few studies on rainfall induced landslides are based on comprehensive~~inventories~~, event-inventories. Some studies are based on individual landslide information. For example, Saito et al. (2014) studied 4744 landslides in Japan, that occurred between 2001 and 2011, to better understand which rainfall property controls landslide size. This dataset, aggregating small subset of the landslides triggered by rainfall events, misses the vast majority of landslides (for example, in Japan, Typhoon Talas alone caused a similar amount of landslides in a few days). It is therefore insufficient for more advanced statistical analyses. At global scale, Kirschbaum et al. (2009), presented a catalog containing information on 1130 landslide events worldwide, occurring in 2003, 2007 and 2008. With this catalog they underlined the correlation between extreme rainfall and landsliding (Kirschbaum et al., 2012). However, such catalogs, mainly based on reports from various kinds, gather very fragmentary knowledge, and contain little quantitative information on landsliding. Thus, we consider that neither ~~landslide scale or global scale studies are sufficient~~ studies based on small sample of individual landslide or on global-scale analysis will be able to constrain effectively Eq 1, and that storm scale detailed information ~~are~~ is needed.

Although relatively rare, some case studies ~~at the catchment scale~~ based on fragmentary event inventories exist (and are briefly reviewed in the next section) but they ~~rarely constrain the whole region affected by the storm, and thus~~ may contain too few landslides for statistical analyses or may be biased to specific locations (e.g., along roads or near settlements, within weak lithological units, near rivers), thus complicating the deconvolution of forcing and site influences. However, in theory, satellite imagery allows comprehensive mapping of landslides larger than the resolution limit, across all catchments affected by a large storm. In practice, obtaining useful images strictly constraining the landsliding caused by a single storm is not always possible, mainly because of cloud coverage, and detailed mapping across vast areas represent a significant work effort. As a result, landslide inventories triggered by rainfall during a whole season or a few years are used for testing mechanistic models (e.g., Baum et al., 2010; Arnone et al., 2011).

The purpose for this ~~paper~~ work is to present a compilation of new and past comprehensive rainfall-induced landslide (RIL) inventories, each ~~representing adequately~~ containing the landslide population associated with an identified storm. They constitute the core of an expandable database, essential for further research. We first briefly review existing comprehensive and partially complete inventory associated with specific storms. Then we present six new inventories and analyze their statistical properties in terms of size ~~, geometry and~~ (total area, landslide density), geometry (length, width and depth) and relation to topographic slopes. We further analyze and discuss the properties relative to rainfall observations in those cases and conclude on the various insights that can be derived from such inventory compilation.

2 Data and methods

2.1 Review of pre-existing ~~dataset~~datasets

An in-depth literature review revealed that very few comprehensive, digital, RIL inventories have been published, such as the Colorado 1999 and Micronesia 2002 events detailed below. If we look for partial inventories, in which landslides have been mapped comprehensively in limited zones affected by a storm, a few more datasets exists.

For example, hurricane Mitch hit central America at the end of 1998 and triggered thousands of landslides across several countries. The rainfall ~~were~~ was record breaking in many places, with rain gauges recording up to 900, 1100 and 1500 mm in Honduras, Guatemala and Nicaragua (Bucknam et al., 2001; Cannon et al., 2001; Crone et al., 2001; Harp et al., 2002). In the following weeks, the USGS performed an number of air-surveys, identified the most affected areas in these three countries as well as in El Salvador (where the rainfall amount was less), and mapped a large number of the failures based on aerial photographs. The resolution of the optical imagery allowed to distinguish failures down to a relatively small size (~~$< 100 m^2$~~ < 100 m^2), but the mapping amalgamated multiple failures into single polygons, and combined very long debris flow paths and/or channel deposits to the source areas. Last, the mapping was only performed in a number of isolated areas, that were "the most affected", and it is unclear how much landsliding was present in the unmapped zones. Because of these limitations, we did not investigate this case in ~~details~~ detail here but note that these inventories may be corrected and used by later studies. Similarly in a number of studies, inventory of all the landslides caused by a given storm in a specific catchment or geographic zone can be found, in Liguria 2000 (Guzzetti et al., 2004), Umbria 2004 (Cardinali et al., 2006), Sicily 2009 (Ardizzone et al., 2012), Peru 2010 (Clark et al., 2016), Thailand 2011 (Ono et al., 2014) and Myanmar 2015 (Mondini, 2017) and in Taiwan for ten typhoons between 2001 and 2009 (Chen et al., 2013). ~~The issues for these partially complete datasets is whether or not the statistical properties of the subset are representative of the entire dataset associated with the stormand its specific properties. There is no doubt that a number~~ These inventories could not constrain the total landslide response to a storm, but may allow to constrain relationships between landslide properties and local rainfall properties, provided that enough landslide have been mapped for statistical analysis (e.g., >50-100) and without any systematic sampling bias. However, a detailed assessment of these datasets ~~could be completed based on available satellite imagery and later complement the database presented here~~properties and of their relation to rainfall is out of the scope of this study although it would probably complement interestingly our work in the future.

In this study we analyzed two datasets published previously by the USGS. First, an afternoon rain on the 28th of July 1999 that triggered numerous landslides and debris flows in the Colorado front range (Godt and Coe, 2007). Based on aerial photographs interpretation and field inspection, landslides were mapped as polygons containing source areas, debris flow travel and deposition zones. Initiation point were assumed to be the highest point upslope of each mapped landslides. In 57 out of 328 polygons ~~were associated to multiple sources~~ multiple initiation points (2 to > 15) ~~. Often~~ were mapped for multi-headed polygons (Godt and Coe, 2007) . These polygons are among the largest of ~~these polygons~~ the inventory and represent 61% of the total landslide area. ~~As the~~ The surface of the source areas were often of similar width, ~~we decided to conserve multi-headed~~

~~polygons and to consider each sources contributed equally~~suggesting equivalent contribution from each source to the transport and deposit areas, and rendering a manual splitting impractical. Thus, we instead conserve multi-headed polygons and we use the whole landslide area, A_l, perimeter, P_l, and number of source, N_s, for each multi-headed polygon to derive an equivalent area and perimeter associated with each source: ~~$A_s = A_l/N_s$~~ $A_l^* = A_l/N_s$ and $P_s = P_l/N_s$. This first order approach underestimates the perimeter of each components by one width (the segment that would be added for each necessary split), however this underestimation decreases with the length/width ratio of the polygons, and is already below 10% for $L/W > 4$. In any case, this assumption does not affect the total area affected, but it changes the landslide frequency-area and frequency-width distributions, and all terms derived from them.

The second dataset contains landslides caused by a summer typhoon in July 2002, mapped exhaustively with aerial photos on the islands of Micronesia (Harp et al., 2004). We digitized the original maps based on strong contrast between red polygons and the rest of the maps. A few artifacts due to this image processing were removed and a few amalgams were split. Again, scarps and deposits are not differentiated.

2.2 New comprehensive inventories of rainfall-induced landslides

We present the mapping methodology and imagery (Table Suppl. 1) used to produce six additional inventories. Here we consider landslides as a rapid downslope transport of material, disturbing vegetation outside of the fluvial domain, which we define by visible water flow in the imagery. We also consider individual landslides with a single source or scar areas to avoid amalgamation, and split polygons when necessary. Although the transition between hillslopes and channel may be blurry and in part subjective, the width estimation (cf 2.4) will mitigate variations of the transport length, as long as large alluviated, or flooded areas are not mapped as landslide deposits. Still the limit between scar, transport and deposit areas could rarely be detected with the available imagery, and all polygons consider the whole disturbed areas on the hillslopes. Subset of the inventories in Taiwan 2009 and Brazil 2011 were produced with automatic algorithm, and then edited and corrected manually, while all others were manually mapped.

In 2008 around the Brazilian town of Blumenau, several days of intense rainfall at the end of a very wet fall triggered widespread landsliding and flooding, with some partial inventories published in the Brazilian literature (e.g., Pozzobon, 2013; Camargo, 2015) but no analyses in the international literature. The detection and manual mapping of landslides as georeferenced polygons was primarily done with a pair of Landsat 5 cloud free images (02/01/2009 and 03/02/2008). The coarse resolution (~~30m~~30 m) of the images allowed only to locate vegetation disturbances and accurate landslide delineation was only possible for the largest events. Therefore we used extensively high-resolution imagery available in Google Earth (over $> 90\%$ of the AOI) acquired in May-June 2009 ~~, and when not available~~ in most areas, and in 2010-2012 elsewhere, where scars were still visible. ~~We~~ To avoid mapping post-event landslides, we mapped only the ones corresponding to vegetation radiometric index (e.g., NDVI) reduction for the pair of Landsat 5 images~~.~~, present even for sub-pixel landslides (e.g., 10x5m). Thus the landslide mapping could be confirmed for ~90% of the mapped polygons, and man-made digging or deforestation occurring on steep slopes could be avoided. This approach avoid amalgamating groups of neighboring landslides and to map very small landslides (~1 pixel in Landsat 5 images). However, some detailed field mapping in the surrounding of Blumenau reports up to

twice ~~more landslides than~~ the number of landslides that we observed (Pozzobon, 2013) indicating that we still miss a number of small events. Nevertheless, these landslides must be quite small (not visible in ~~$\sim 1m$~~ $\sim$ 1 m resolution imagery) and likely do not affect any of our statistics (area, volume, slope) apart the total number of landslides.

The same approach was used to map the intense landsliding caused by a few days of intense rainfall between the 10^{th} and the 12^{th} of January 2011 (Netto et al., 2013), in the mountains northeast of Rio de Janeiro. Near Teresopolis, we used first a pan-sharpened (~~10m~~10 m) EO-ALI and a 30 m Landsat 7 images from February 2011 for co-registration and ortho-rectification. $> 95\%$ of the slides were cross-checked in Google Earth based on images from the 20th and 24th o fJanuary 2011 (Fig 1) and where clouds or no images where available we mapped landslides directly from Google Earth (available over >90% of the AOI), even if poor ortho-rectification may create geometric distortions. Closer to Nova Friburgo, we used a pair of very high resolution Geoeye-1 image ~~presented in Stumpf et al. (2014) , and extended the methods presented in their study~~ (2/0.5 m resolution in multispectral/panchromatic) from the 26th of May 2010 and the 20th of January 2011. On these images we applied the methods presented by Stumpf et al. (2014) , to classify the whole image~~. Then~~, detecting $> 90\%$ of the landslides we could observe manually, but also including false positive. Thus, we screened manually the image to remove ~~false positive (~~agricultural field, inundated areas, channel deposits ~~)~~ that were included and split the amalgamated landslides, very frequent given the important clusters of landslides in many part of the image. This correction seems sufficient given that landslide size distribution for the three subparts of the inventory are consistent (Fig. Suppl. 1). Polygons from the automatic classification display a slightly larger equivalent length/width ratio, maybe because some amalgamated polygons have been missed or simply because the classification allows hollow polygons, biasing upward the length/width estimate based on a perimeter/area ratio (~~see below~~cf 2.4).

In the first days of September 2011 (1st-4th), typhoon Talas triggered very heavy rainfall on the Kii Peninsula, in Japan, resulting in several thousands of landslides. For disaster emergency response, the National Institute for Land and Infrastructure Management of Japan mapped landslides across most of the affected areas based mainly on post-typhoon aerial photographs and occasionally on Google Earth imagery (Uchida et al., 2012). Screening antecedent imagery (2010-2011) from Google Earth and Landsat 5 we identified and removed a few hundreds pre-Talas polygons, mostly within ~~5km~~ 5 km of 136,25°E/34,29°N and 135,9°E/34,20°. With Google Earth we could validate NILIM mapping over about 85% of the AOI and we added almost 200 polygons in areas were aerial photographs were not taken, and split many large or multi-headed polygons that were amalgamated. Some polygons had distorted geometry or exaggerated width, most likely due to poor ortho-rectification of the aerial imagery and/or time-constrains for the mapping. We could not systematically check all polygons, but we checked and corrected all polygons larger than $30,000m^2$ (3% of the catalog but representing 45% of the total area). We consider that the remaining distortions for some of the smaller polygons have minor impacts on the statistics discussed in the next sections.

In Taiwan, we collected landslide datasets associated with the 2008 Kalmaegi (16-18th Jul.) and 2009 Morakot (6-10th Aug.) typhoons, partially described by Chen et al. (2013). For 2008, we compared multispectral composite images and NDVI changes between (30 m) Landsat 5 images taken on the 06/21, 07/07 and 07/23. The image from 07/07 is covered by clouds and light fog in many parts but allows identifying that most places affected by landslides in the last images were still vegetated at this time. Thus all new landslides ~~, delineated manually,~~ are attributed to the rainfall from typhoon Kalmeagi. For 2009, landslides were

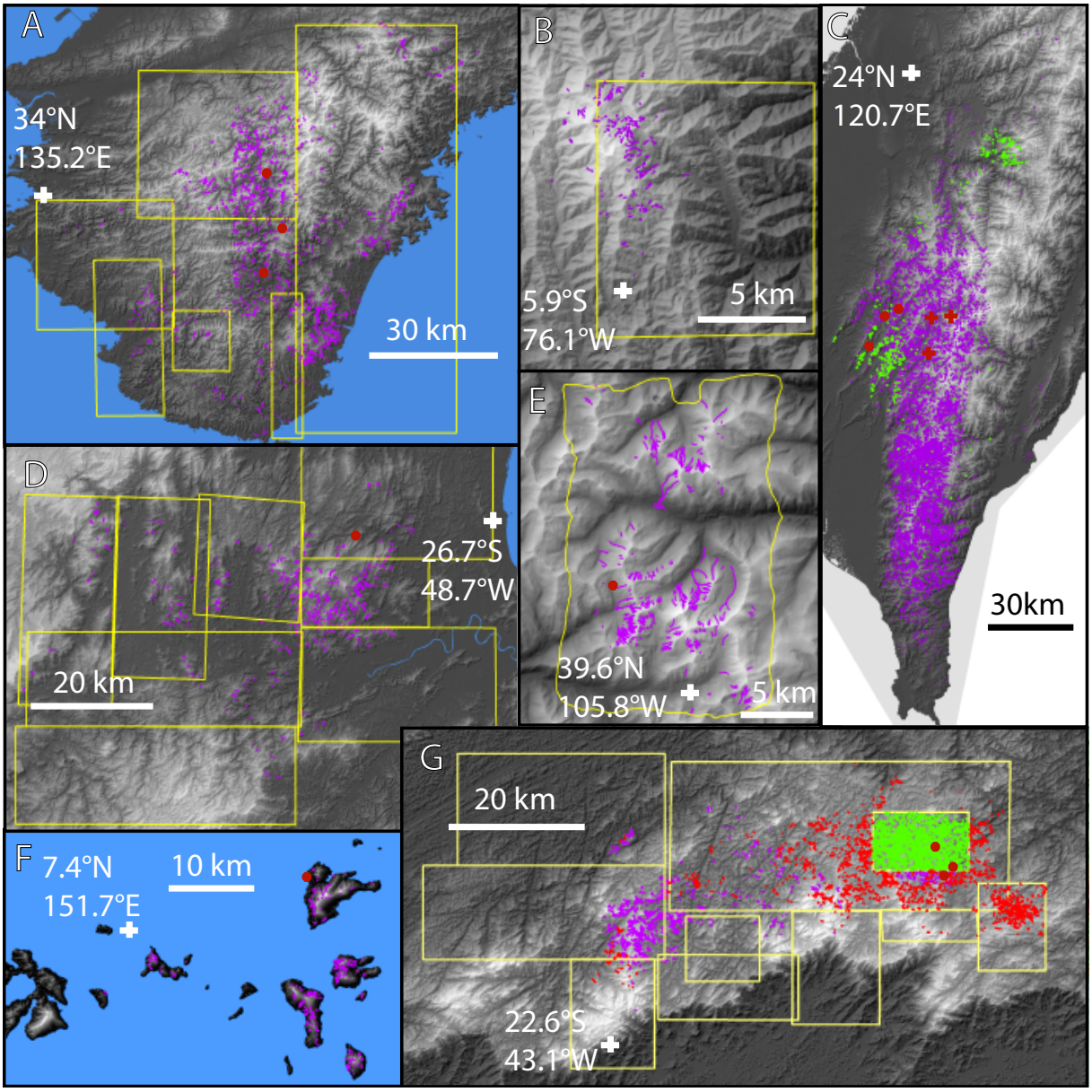

Figure 1. Landslides inventory superimposed on digital surface model for the events in Japan 2011 (A), Brazil 2008 (B), Micronesia 2002 (C), Colombia 2015 (D), Colorado 2002 (E), Brazil 2011 (F) and Taiwan 2008 and 2009 (G). Landslides are in purple, rain gauges used in this study are in red dots (and red crosses for Taiwan 2009), and the yellow frames show the availability of high resolution imagery (Google Earth) used to check or perform the mapping. In G, the pink dots are landslides from 2008, while purple dots are from 2009. In F, purple, pink and cyan are landslides mapped from EO-ALI, Google Earth and automatic classification of Geoeye image, respectively.

~~delineated manually by comparing surface reflectivity and morphology on~~ mapped with pre- and post-event FORMOSAT-2 satellite images (2 m panchromatic and 8 m multi-spectral) (Chang et al., 2014). To cover most of the island, we mosaicked multiple mostly cloud-free pre-event (01/14, 05/08, 05/09, 05/10, 06/06 of 2009) and post-event (08/17, 08/19, 08/21, 08/28, 08/30, 09/06 of 2009) images. For ~~sub-parts~~ subsets of the inventory, especially to the East of the main divide, landslides were ~~first mapped automatically and then edited manually. For both approaches, the scar, runout and deposit areasare not differentiated. We did not consider debris flow transport within the fluvial system and ignored gentle slopes ($< 10°$) from mapping to avoid confusion with human activity.~~ significantly amalgamated and bundled with river channel alluviation. We thus manually split the polygons and removed the channel areas. In a few areas with clouds ($< 5\%$ of the AOI) in the post-event mosaic, we ~~used Landsat imagery to be sure to map at least the largest landslides~~ mapped with Landsat 5 images (from 24th of June and 12th of September 2009), even if the spatial resolution limit may have censored the smallest landslides in these zones. Special attention was given to the separation of individual landslides by systematically checking and splitting polygons above ~~$0.1km^2$~~ 0.1 km^2 (2% of the catalog but representing 30% and 60% of the total area and volume). However, it is clear that a number of smaller slides are missed or merged with large ones, and therefore although total landsliding and landslide locations on slope may be well represented, the size distribution of this catalog must be biased to some extent.

Between 15 and 17th of May 2015, heavy rainfall in the mountains above the village of Salgar, Colombia, triggered catastrophic landslides and debris flow (>80 deaths). Landslide mapping was carried out by comparing a (10 m) Sentinel 2 image from the 21st of July 2016 ~~to a 2014~~ and a pan-sharpened (15 m) Landsat 8 image ~~.~~ from the 19th of July and 26th December of 2014. These images were selected for their absence of clouds, good conditions of light and similarity. ~~Other intermediate images in between those show very little activity before or after May, supporting the idea that all mapped landslides can be attributed to this single~~ High spatial resolution imagery from Google Earth, dated from the 31st of May 2015 shows fresh scars consistent with our mapping over most of the area (Fig 1), and we assumed that the remaining landslides ($< 15\%$ of the inventory) were also triggered by the same rainfall event.

2.3 Rainfall data

Rainfall data quality and amount are very variable for the different events, from 0 or 1 single gauge (For Micronesia or Colombia), to dense gauge network and potentially weather radar coverage in Japan, Taiwan and Brazil. Therefore we selected a simple index that could be obtained for each case in order to discuss potential rainfall controls on the landslide properties. For each case we calculated an estimate of total rainfall, R_t, duration, D, and a peak rainfall intensity over 3 hours, $I3$ (Table 1). Note that these variables do not represent an average value within the whole footprint of the storm~~but rather~~ , but rather a maximal forcing, usually colocated with the areas where landsliding was the most intense (Fig 1) ~~,~~and derived mostly from one or a few rain-gauges. Thus these indexes may be taken as a storm magnitude. A more detailed analysis of the spatio-temporal pattern of the rainfall and of its relations to the spatial pattern of landsliding is highly desirable, but challenging ~~with the available dataset. Indeed, some cases with little in-situ information may be best studied by a combination of meso-scale rainfall modeling possibly assisted by satellite information, while other would require integration and processing of extensive rain-gauges and radar measurements. For this study, we limit our scope to the analysis of specific landslide behavior and to~~

~~the proposition of a series of research hypotheses that could be later investigated with very detailed inventories and adequate rainfall analyses~~and is left for a future study.

The estimates from Taiwan and Japan are based on hourly gauge measurements from the Japan Meteorological Agency and Taiwan Institute for Flood and Typhoon research. In each case we took the three closest gauges within 5 to ~~15km~~ 15 km from the areas with the highest landslide densities (in 0.05 by 0.05° window) (Fig Suppl. 2) and computed their average ~~record~~ properties (Fig 2). Minimum and maximum single gage measurements give a coarse measure of the uncertainty. A single gauge is available in Micronesia and we used the hourly rainfall from 1st to 3rd of July 2002 reported in Harp et al. (2004). For Colorado, we used the hourly rainfall from the rain gauge at Grizzly peak, closest ~~of~~ to intense landsliding and reported by Godt and Coe (2007). For ~~the~~ this event radar data indicates very localized high intensity precipitation located on the peaks where the debris flows occurred (Godt and Coe, 2007)) and suggests that the single closest gauge is more representative than averaging with the other nearby ones. For the event in Brazil 2008 we considered the total daily rainfall from Luis Alves station (Fig 1), where more than ~~130mm~~ 130 mm per day were accumulated on the 21^{st}, 22^{nd} and 23^{rd} of November and ~~250mm~~ 250 mm on the 25^{th}, and intensity going up to ~~50mm~~50 mm/hr (Camargo, 2015). These days were also preceded by abnormally wet period, with November 2008 accumulating ~~$\sim 1000mm$~~ $\sim$ 1000 mm, 7 times the long term average for this month. In 2011 in Brazil, hourly rain data at Sitio Sao Paulista reports 200 mm in 8 hours before gauge failure, while there and at nearby sites, the cumulative rainfall was ~~$\sim 280mm$~~ $\sim$ 280 mm from the 10th to the morning of the 12th January (Netto et al., 2013). For these cases, raingages give a trustworthy estimate of the local rainfall, but are not constraining the large scale rainfall pattern. Last, in Colombia, we could not find data from any nearby rain-gauge and we thus use rainfall estimates from the GSMaP global satellite products (Kubota et al., 2006; Ushio et al., 2009) (Fig Suppl. 3). Here, the minimum, mean and maximum rainfall are obtained by considering the triggering storm as the raining period at the time of debris flow occurrence, or the one from the previous day or merging both events, respectively (Fig Suppl. 3).

Defining storm duration accurately requires defining thresholds on rainfall intensity ~~other~~ over given periods, to delimit the storm start and end. Given the variable quality of our data we limit ourself to a first order estimate of the continuous period when rainfall was sustained ~~.~~ (i.e., $I3 > 3$ mm.hr^{-1}). We consider these durations accurate within 10-20% for the events with overall hourly data. For the less constrained cases B08, B11 and C15 duration is more uncertain. In any case, for these 8 storms, we note a strong correlation between D and R_t and $I3$ and R_t (for power-law scalings, ~~$R^2 = 0.8$ and $R^2 = 0.7$, respectively~~ $R^2 = 0.9$ and $R^2 = 0.8$, respectively (Fig Suppl 4). Thus, given that spatial and temporal length scales are often linked in meteorology, the long events causing larger rainfall may also have larger footprints.

2.4 Landslide area, width and volume

Landslide planview area and perimeter are directly obtained from each polygon. However, these values represent the total area disturbed, that is the scar, deposit and runout areas, because a systematic delineation of the scar was not possible from most of the imagery. This means that landslide size statistics ~~is~~ are resulting from processes affecting both landslide triggering and runout. Landslide volume, estimated based on area, may also be overestimated for long runout slides. Therefore we propose

Table 1. Rainfall data summary, containing the total rainfall, duration and maximum 3-hours intensity for each storms. For TW8, TW9 and J11, we indicate the range for the three indexes that could be estimated from three gauges near the zone of maximal landsliding. We cannot perform this analysis for MI2 and C99, and can only assess a range of R_t for B08 and B11. For C15, we indicate by a star that we could only access satellite based rainfall estimates (GSMaP version 7 ungauged products, see Fig Suppl. 3). Reference are as ~~follow~~follows, 1: (Godt and Coe, 2007), 2: (Harp et al., 2004), 3:(Camargo, 2015) , 4:(Netto et al., 2013) .

Event	C99	MI2	B08	TW8	TW9	B11	J11	C15
R_t, mm	45	500	695[680-800?]	670[600-740]	2500[2100-2800]	280[200-320]	1300[1000-1500]	65[10-75]*
D, hours	4	20	100	24	~~100~~ 105	36	~~65~~ 62	10*
$I3$, ~~$mm.hr^{-1}$~~ $mm.hr^{-1}$	13	65	30	92[78-116]	85[83-87]	55	58[38-88]	8*
Ref.	1	2	3	Us	Us	4	Us	GSMaP

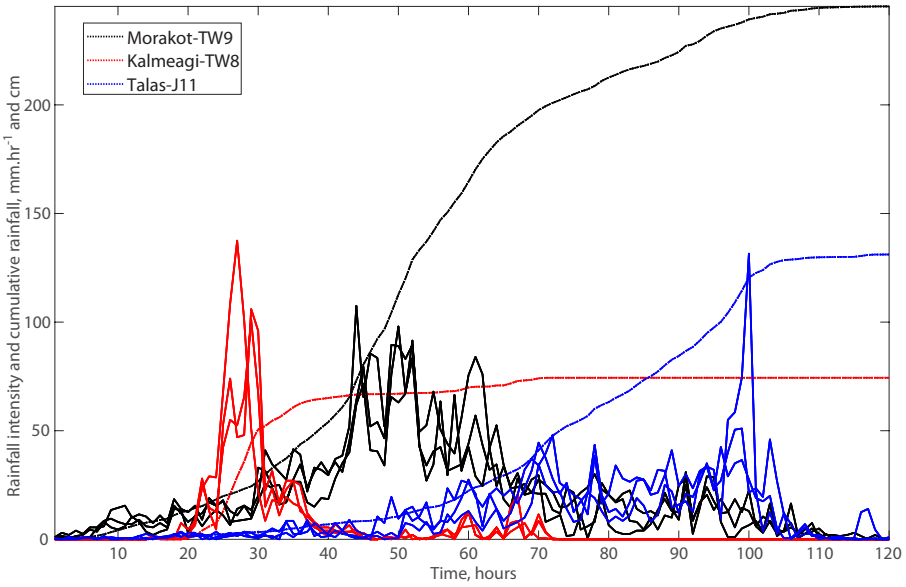

Figure 2. Rainfall history for typhoons Kalmaegi (TW8), Morakot (TW9), Talas (J11). For each event, hourly intensity is shown with solid curves for three gauges nearby the area with most intense landsliding (see Fig 1 for locations). Dashed lines represent the mean cumulative rainfall from the three gauges.

here a simple way to normalize for landslide runout and obtain an estimate of the scar area.

Following Marc and Hovius (2015), we computed an equivalent ellipse aspect ratio, ~~K~~K, using the area and perimeter of each polygons. For ~~polygons~~ polygon with simple geometries, ~~K~~ K is close to the actual length/width ratio, but this is a measure that also increases with polygon roughness or branching, and therefore with amalgamation (Marc and Hovius, 2015). ~~An ellipse~~ Assuming an elliptic shape, polygon area can be approximated by $\pi LW/4$ with L and W being the ~~polygons~~ polygon full length and width, respectively. This allows us to estimate $W \simeq \sqrt{4A/\pi K}$. ~~Again, this value is close to the actual mean width of polygons that do not have artifacts. Thus~~To validate this geometric method to retrieve landslide width, we measured systematically the width of 418 randomly selected landslides across a wide range of polygon areas and aspect ratios, belonging to four inventories: J11, TW8, B11, and C15. For each polygon, we focused on the upper part of the landslide only, the likely scar, and averaged 4 width (i.e., length perpendicular to flow) measurements made in arcGIS. The width estimated based on P and A are within 30% and 50% of the measured width for 72% and 92% of the polygons, respectively (Fig Suppl 5).We do not observed a trend in bias with area nor aspect ratio, except perhaps for the automatically mapped landslide in B11, where high aspect ratio correlates with underestimated width. Thus, for correctly mapped polygons we can use ~~width to derive~~ P and A to derive W and a proxy of landslide scar area, ~~$A_s \sim W^2$. Although~~ $A_s \sim 1.5W^2$. We assume landslide scars have an aspect ratio of 1.5, as it was found to be the mean aspect ratio found across a wide range of landslide size within a global database of 277 measured landslide geometries (Domej et al., 2017) . Even if this equivalent scar area may not exactly correspond to the real landslide scar, it effectively removes the contribution of the landslide runout to the landslide size and allows to compare different size distributions while reducing the impact of variable runout distances.

We also assessed how using A_s affects estimates of landslide volumes and erosion, by computing landslide volume with the total landslide area and with A_s only. In both cases, we used $V = \alpha A^{\gamma}$, with α and γ and their 1σ globally derived by Larsen et al. (2010). Given that soil and bedrock slides have different shape and that soil slides are rarely larger than ~~$10^5 m^2$ ($10^4 m^2$~~ 10^5 m^2 (10^4 m^2 for soil scars) (Larsen et al., 2010), we used the "all landslide" parameters ($\gamma = 1.332 \pm 0.005$; $log_{10}(\alpha) = -0.836 \pm 0.015$) when $A < 10^5$, and the "bedrock" parameters ($\gamma = 1.35 \pm 0.01$;$log_{10}(\alpha) = -0.73 \pm 0.06$) for larger landslides. Similarly we used the soil scars ($\gamma = 1.262 \pm 0.009$; $log_{10}(\alpha) = -0.649 \pm 0.021$) and bedrock scars ($\gamma = 1.41 \pm 0.02$; $log_{10}(\alpha) = -0.63 \pm 0.06$) for ~~$A_s < 10^4\ m^2$ and $A_s >= 10^4\ m^2$~~ $A_s < 10^4$ m^2 and $A_s >= 10^4$ m^2, respectively (Larsen et al., 2010). Marc et al. (2016) proposed a rudimentary version of such a runout correction, where they effectively reduced landslide area by a factor 2 for mixed landslides and 3 for bedrock landslides, noting that volumes derived in this way were closer to field estimates for large landslides than without correction.

Uncertainties in this approach include the 1σ variability of the coefficient and exponent of the landslide area-volume relations given above, and an assumed standard deviation of 20% of the mapped area. These uncertainties were propagated into the volume estimates using a Gaussian distribution. The standard deviation on the total landslide volumes for the whole catalogs or for local subsets, were calculated assuming that the volume of each individual landslide was unrelated to that of any other, thus, ignoring possible co-variance. Although estimated 2σ for single landslides is typically from 60 to 100% of the individual volume, the 2σ for the total volume of the whole catalog is below 10% for the eight datasets. However, for subset with ~~less~~ fewer landslides and with volume dominated by large ones, typical when we compute the total landslide volume density in

small area (e.g., 0.05°), 2σ ~~uncertainties~~ uncertainty reaches 40-60%. We note however, that these uncertainties estimates do not consider potential errors in the identification of landslides, either missed because of occasional shadows or clouds or erroneously attributed to the storm. Such uncertainty is hard to quantify but must scale with the area obscured in pre- and post-imagery. In most cases multiple pre- and post-event images mean that obscured areas represent typically less than 10% of the affected area, and such errors may be between few to $\sim 20\%$ of the total area or volume, depending on whether obscured areas contain landslide density higher or lower than the average observed throughout the affected area. Last, resolution may not allow to detect the small landslides and in some cases the landslide number may be significantly underestimates, but not the total area and volume dominated by the larger landslides.

Last, for each inventory, we estimated the landslide distribution area, that is the size of the region within which landslide are distributed. Based on the landslide inventories we could delineate an envelope containing the overall landsliding. As discussed by Marc et al. (2017), such delineation is prone to high uncertainties as it is very dependent on individual isolated landslides. Thus for all cases, we give a range of distribution area, where the upper bound is a convex hull encompassing all the mapped landslides, while the lower bound is an envelope ignoring isolated and remote landslides ~~,~~ (i.e., single or small cluster of landslides without other landslides within 5-10 km), if any. Although the spread can be large in absolute value, both approaches yield the same order of magnitude.

3 Results

The ~~built~~ inventories contain from ~~$\sim$ 100 to $>$ 15,000~~ $\sim$ 200 to $>$15,000 landslide polygons, representing total areas and ~~volumes from 0.2 to 200km^2 and 0.2 and 700Mm^3~~total volumes (from scars) from 0.2 to 200 km^2 and 0.3 to 1000 Mm^3, respectively. The triggering rainfalls are characterized by a total precipitation of ~~$\sim$ 50~~ $\sim$ 50 to 2500 mm in period ranging from 4h to 4 days, and caused landslides within areas ranging from ~~$\sim$ 50 to 10,000km^2~~$\sim$ 50 to 10,000 km^2. Although the dominant landslide types are soil and regolith slumps, a number of large deep-seated bedrock landslides are also present in the inventories associated to the Talas and Morakot typhoons (Saito and Matsuyama, 2012; Chen et al., 2013). A more detailed description of the landslide types and materials involved was not possible with the available imagery; thus our analysis does not consider landslide types. In the next sections, we present results obtained from these inventories in terms of landslide size statistics, landslide spatial patterns and relation to slope, before correlating these landslide properties to rainfall parameters.

3.1 Landslide properties

3.1.1 Landslide size statistics

Frequency size distribution of landslide inventories ~~typically have power law, heavy-tail,~~ have typically been fit by power-law tailed distributions, above a certain modal size (Hovius et al., 1997; Malamud et al., 2004). The modes and the decay exponents of these distributions are mainly related to the lithology (mechanical strength) or topographic landscape properties (i.e., susceptibility related) (Stark and Guzzetti, 2009; Frattini and Crosta, 2013; Katz et al., 2014; Milledge et al., 2014). Some au-

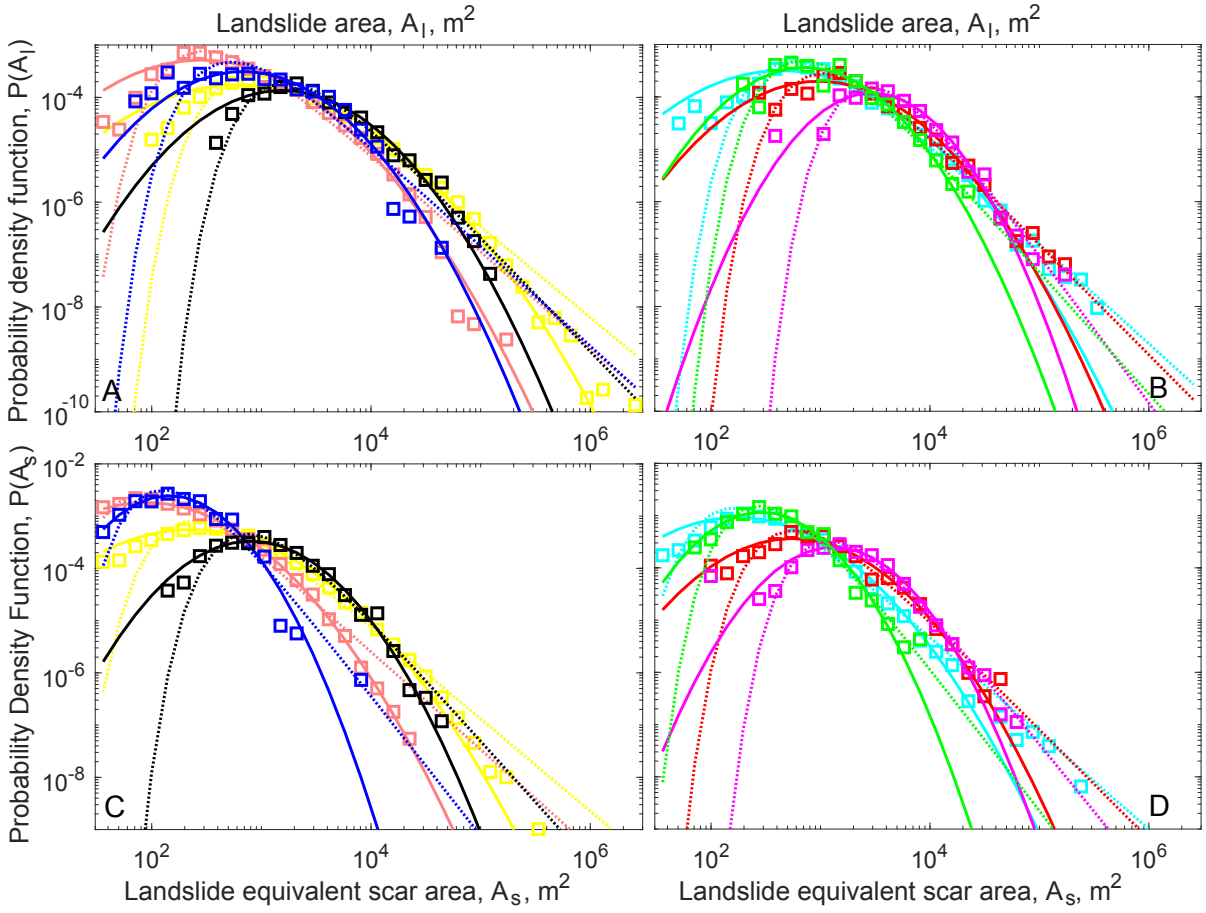

Figure 3. Probability density functions of landslide whole area (A, B) and estimated scar area (C, D). ~~A least square power-law fit of~~ To improve visualization we split the ~~tail~~ 8 inventories in two groups. A Log-Normal and ~~an IGD~~ Inverse Gamma Distribution maximum-likelihood estimation for the whole distribution are shown by solid and dashed lines respectively.

thors suggested that this behavior could also be affected by the forcing processes. For example analyzing earthquake induced landslide catalogs, it was found that deeper earthquakes, thus with weaker strong-motions, have a smaller proportion of large landslides (Marc et al., 2016). Based on theoretical arguments, it has been proposed that short high intensity rainfall could cause pulses of high ~~pore water~~ pore-water pressures at the soil-bedrock transition, initiating mainly small shallow landslides, while, long duration rainfall with ~~important~~ large total precipitation could provoke significant elevation of the water table and trigger large, deep-seated landslides (Van Asch et al., 1999). To our knowledge, only few empirical evidences have supported these assumptions, and we discuss next how our data compare to these ideas.

All landslide size distributions present a roll-over and then a ~~decay that may be fitted by a negative power-law function~~ steep decay (Fig 3). The modal landslide area varies between ~~$\sim 3000\ m^2$~~ $\sim$ 3000 m^2 for TW8 and ~~$\sim 300\ m^2$~~ $\sim$ 300 m^2 for B11,

while the largest landslides are ~~$\sim 0.1\ km^2$~~ ~ 0.1 km^2 for most events and reach ~~~ 0.4 and $2.8\ km^2$~~ ~ 0.4 and 2.8 km^2 for J11 and TW9, respectively. The roll-over position certainly relates partly to the spatial resolution and acquisition parameters of the images (Stark and Hovius, 2001)(e.g., for TW8 and B08 where landslides where mostly mapped on coarse spatial resolution image compared to aerial photographs for C99, J11). However, ~~physical parameters must also control~~ mechanical parameters are also expected to influence the roll-over position ~~given that, for example,~~ (Stark and Guzzetti, 2009; Frattini and Crosta, 2013) , as suggested by the fact that MI2, mapped with 1m resolution aerial imagery, has larger modal area than C15 mapped with 10 m Sentinel-2 satellite imagery. ~~The fit of the power-law decay beyond the mode or of the whole distributions with an Inverse-Gamma~~ Following Malamud et al. (2004) we use maximum likelihood estimation (MLE) to fit the whole distribution with an inverse gamma distribution (IGD) ~~(cf, Malamud et al., 2004) gives decay exponents ρ between~~ and obtain power-law decay exponents $\alpha + 1$ between ~ 2 and 3, consistent with the typical range found in the literature (Hovius et al., 1997; Malamud et al., 2004; Stark and Guzzetti, 2009; Frattini and Crosta, 2013). However, we note that at least three cases, B11, TW9 and C99, ~~have peculiar distributions~~poorly follow an IGD, with a break in the distribution occurring at large areas, ~~and~~ followed by a very steep decay. ~~For these cases, the IGD gives a rather poor fit for the largest areas, and the normalized difference in decay exponent between a least-square fit of the tail and the IGD maximum likelihood is larger than the typical $\sim 10\%$ uncertainties on the exponent determination (21, 25 and 66% respectively, against $6 \pm 5\%$ for the five other cases).~~

When considering landslide estimated scar sizes, that is essentially a correction to reduce landslide polygon aspect ratio ~~below 2~~to 1.5, we observe a reduction of the largest landslide size by 2 to 10 fold, but a moderate reduction of the ~~mode size~~modal area. This is consistent with the fact that landslides with long runout distances are often over represented within the medium to large landslides (Fig Suppl ~~4~~6). We also note that after the runout distances variability is normalized, the ~~peculiar size~~ distribution of C99 ~~disappears and least-squares fits and IGDgive decay exponents identical within a few percent~~agrees better with an IGD. This is not the case however for B11 and TW9 that still feature a steepening of their distribution decay (and a divergence from IGD fit) beyond $\sim 10^3$ and ~~$\sim 10^4\ m^2$~~ $\sim 10^4$ m^2, respectively. Runout being normalized, this could be an artifact relating to residual amalgamation for TW9, but not for B11 where most landslides were mapped manually and amalgamation was avoided. ~~Thus, this peculiar distribution may be the fingerprint of some physical phenomena but no reasonable hypotheses may be assumed so far~~In these two cases, for the whole landslide area or the landslide scar only, we note that a MLE fit of a log-normal distribution agrees better to the data (based on the result of both the Kolmogorov-Smirnov and the Anderson-Darling test). For other inventories a log-normal fit is equivalent or worse than an IGD, but we note that the parameter describing the decay of both distribution are almost perfectly correlated (Fig Suppl. 7). Thus we take $\alpha + 1$ as a reasonable indicator of the relative proportion of large landslides within the different dataset and do not explore further the functional form of landslide size distribution and its implications, which we consider beyond the scope of this study.

3.1.2 Landslide and slope distribution

For all cases, we computed the frequency of slope angles above 5° based on the global 1 arc-second (~~$\sim 30m$~~ ~ 30 m) SRTM digital surface model. In most cases, hillslopes have a distribution clearly independent from valley floors. However, for B08 and MI2 for example, the amount of plains in the study area do not allow to resolve the hillslope distribution. Therefore, for

Micronesia we removed all slopes which are less than 10 m above sea-level, and for Brazil, we extracted the slope cells in the landslide distribution area but with a mask excluding the wide valley bottoms. The slope distributions of , allowing to obtain a hillslope distribution as an approximate Gaussian, with a mode significantly beyond our threshold of 5°. To focus on the scar area of each landslide polygon, we extracted only the slopes for the highest elevation pixels representing a surface of $1.5W^2$. Then, we computed the probability density function for the landslide affected area and the whole topography (hereafter the "landslideaffected areas generally lead to a sparsely populated histogram, " and therefore, to compare it with the topographic distribution, all histograms were smoothed with a moving average in a window of 3° width. "topographic" distributions) with a normal-kernel smoothing with an optimized bandwidth, as implemented in Matlab. We obtain topographic modal slopes, S_M, at 15.5° and 18.5° for the gentle landscape of Micronesia and Brazil, while in Japan and Taiwan we reach almost 30° (Fig 4A). The slope distributions of landslide affected areas are systematically shifted towards steeper slopes. In most cases the landslide distribution has a very small shift, but for the C99, B11 and landslide distributions are unimodal, except for C15 rainstorms the shift is more pronounced with a landslide modal slope ∼5° larger than S_M. We note that , for the landslide distribution, the proportion of slopes gentler than the topographic mode may be exaggerated due to the inclusion of deposition areas. This is most significant for the C99 case, but also possibly affecting MI2 or B11. For C99 we have also extracted the slope at the initiation point and found this distribution to have a similar mode and decay beyond it than the whole landslide distribution (Fig 4)that seems to have secondary modes at $S_M - 5$ and $S_M + 25$, and are systematically shifted towards steeper slopes.

To further quantify the differences in slope sampling between these events, we computed the ratio of probability between the slope distribution of the whole topography and of the landslide affected area only, P_L/P_T (Fig 4). This ratio represents the tendency of landslide occurrence on a given slope to be more or less frequent than the expected occurrence of a slope gradient units this given slope in the landscape. We refer to this as and over an oversampling or undersampling of the topographic slope distribution. To focus on landslide triggering and on the scar areas, we plot this ratio only for $S > S_M$ and against $S - S_M$ to compare the events in different landscape (Fig **??**A). we plot each event against $S - S_M$ (Fig 4B). An important issue is to determine whether the landslide probability can be considered a random drawing from slopes of the topography or not. Given that landsliding affect less than 10% of the landscape, the sampling of the topography by landslides can be approximated by a Bernoulli sampling. In this case, the central limit theorem gives the 95% prediction interval as $P_T \pm 1.96\sqrt{P_T(1-P_T)/N}$, with N the number of independent draws, here taken as the number of landslide scars. The convergence of N draws to P_T within the prediction interval is only valid if $N > 30$, $NP_T > 5$ and $N(1-P_T) > 5$, implying that only very large samples can be interpreted towards the extremity of the topographic slope distribution, where P_T is small.

Most events (in Taiwan, Japan, Micronesia) actually maintain an almost equal sampling across all steep slopes. We neglect the important variations present for some cases at slopes 30 to 40° steeper than S_M, as they may be artifact due to the small absolute number of cells in this value range. However, B08, B11, C99 and C15, diverge strongly from equal sampling. The latter three have a remarkably similar pattern, with undersampling at the mode and a rapid increase with steeper slopes until a 3 to 10-fold oversampling between ∼ 15 and 30° For all events we observe that P_L is significantly different from a random drawing of the topography with oversampling of the slopes beyond S_M . This shows that additionally to a steeper landslide mode, landslides are increasingly more frequent on very steep slopes , typically reaching a maximum of oversampling between 40° and 60°. In

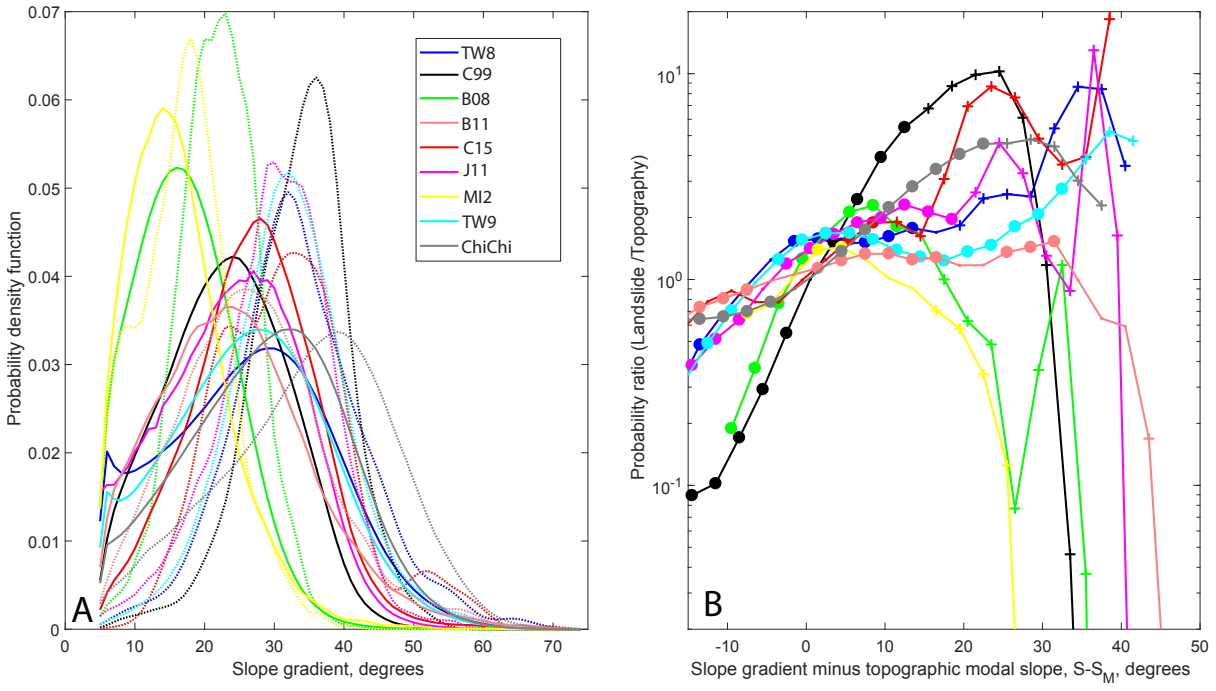

Figure 4. (A) Slope gradient probability distribution for the affected topography (solid) and the ~~landslides affected~~ landslide scar areas only (dashed), for the eight rainfall events and as a comparison to the Chi-Chi earthquake. ~~For C99 we have a~~ (B) Ratio of the two probability distributions against the difference between slope gradient and the modal topography. The ratios are estimated with the PDF averaged within 3° bins. Solid circles and dots represent ratios where the landslide probability is beyond or within, respectively, the 95% prediction interval of the topography distribution. Crosses indicate bins where data are insufficient for the ~~landslide including deposit and for source point only~~validity of the Central Limit Theorem required to estimate prediction interval.

~~contrast, in~~ and undersampling below it (Fig 4B) . However, we note that for most events, the undersampling and oversampling is smaller than a factor of 2. Some cases (C15, J11 and TW8) have stronger oversampling (> 4) for $S - S_M > 25$ but they may not be representative ratios given the limited number of landslides and of slopes thus steep (i.e. $NP_T < 5$). The scars of C99 clearly departs from this behavior, with undersampling and oversampling of a factor of 10 and 6 at $S_M \pm 10$, respectively. B08 ~~we observe undersampling starting at 10° beyond the mode and reaching a 5-10-fold undersampling beyond 20°.~~ has also strong undersampling below S_M but has a landslide distribution that rapidly converges to the topographic ones at high slopes.

~~(A) Ratio of the two probability distributions against the difference between slope gradient and the modal topography. We display two curves for C99 landslides, the dash-dotted one from the whole landslide area, including deposits, and the other from source point only. (B) Anti-correlation between the steep slope sampling (that is the mean of P_L/P_T for $S - S_M$ in $[15, 30]$) and storm duration. Solid and dashed lines are the best power law fit of the data, averaging C99-all and C99 source into 1 data point ($R^2 = 0.7$). We indicate with an arrow that B08 duration may be underestimated.~~

3.2 Correlation between rainfall metrics and landslide properties

3.2.1 Total landsliding

For the eight inventories, we observe a non linear increase of all metrics of total landsliding with the storm total rainfall (Fig 5). The increase is ~~fairly~~ similar for the total area and volume, and best fit by exponential functions. We observe higher correlations with rainfall, when using the total scar area ($R^2 = 0.78$), estimated as W^2, instead of the total area ($R^2 = 0.72$). This is mainly due the very large reductions of area for C99 and B11 where long runout landslides were dominant (Fig 5). Correlation are generally higher with volume and also increase when we derive total volume from scar estimates (from $R^2 = 0.81$ to $R^2 = 0.87$). Note also that with these scar metrics, the relation to rainfall becomes equally or better fit by power-law function rather than an exponential function (Fig 5). This is because when including landslide runout the total landsliding of C99 and C15 is larger and ~~create~~ creates an apparent asymptote, better fit by an exponential function. Last, we note that total volume values may change depending on which A-V scaling relations is used and with which assumptions, and their absolute values may be inaccurate but this should not affect much the reported scaling form and exponents as potential biases should be relatively uniform.

Total number of landslides also tends to increase with total rain but the scatter is much larger (Fig 5). This is at least partly an artifact, given that for C99, MI2 and B11, high spatial resolution imagery allows to delineate many more small landslides and to mitigate amalgamation, whereas for B08, TW8 and TW9, the limited spatial resolution, the density of landsliding and our limited ability to split amalgamated landslides lead to an underestimation of the landslide number. Thus, even if landslide number may contain information, quantitative comparisons of the ~~different~~ events are biased and we will not further interpret the total number of landslides in the following.

Last, we note that the landslide distribution areas (i.e., the regions within which landslides are distributed) also correlate strongly with the total rainfall. Only considering the eight inventories strongly suggest a power law form. However, based on the dataset reported for the Hurricane Mitch, the distribution area was at least 100,000 ~~km^2~~ km^2, for maximum total rainfall at about ~~1500mm~~ 1500 mm (Cannon et al., 2001). Adding it to our fit, we found that power-law or exponential functions of the rainfall explained similar amount of the variance, 72% and 63% respectively.

In the next subsection, we compute landslide densities (in % of area), allowing to study the intra-storm variability of landsliding.

3.2.2 Maximum and mean landslide density

Understanding what controls landslide density is a key objective to better constrain hazards and their consequences. For each storm we compute the mean landslide density (in area and volume) by dividing total landsliding by the landslide distribution area (Fig 6A). This density represents the whole affected area and hides important spatial variability (Fig 1), thus we also compute the maximum landslide density, by computing the total landsliding (again in area and volume) within a moving window of 0.05° (~~$\sim 25 km^2$~~ $\sim$ 25 km^2), assigning landslides to a cell based on their centroid locations, and selecting the maximal value (Fig 6B). Given the better correlation obtained above with a runout normalization, we focus on area and volume densities derived from scar estimates.

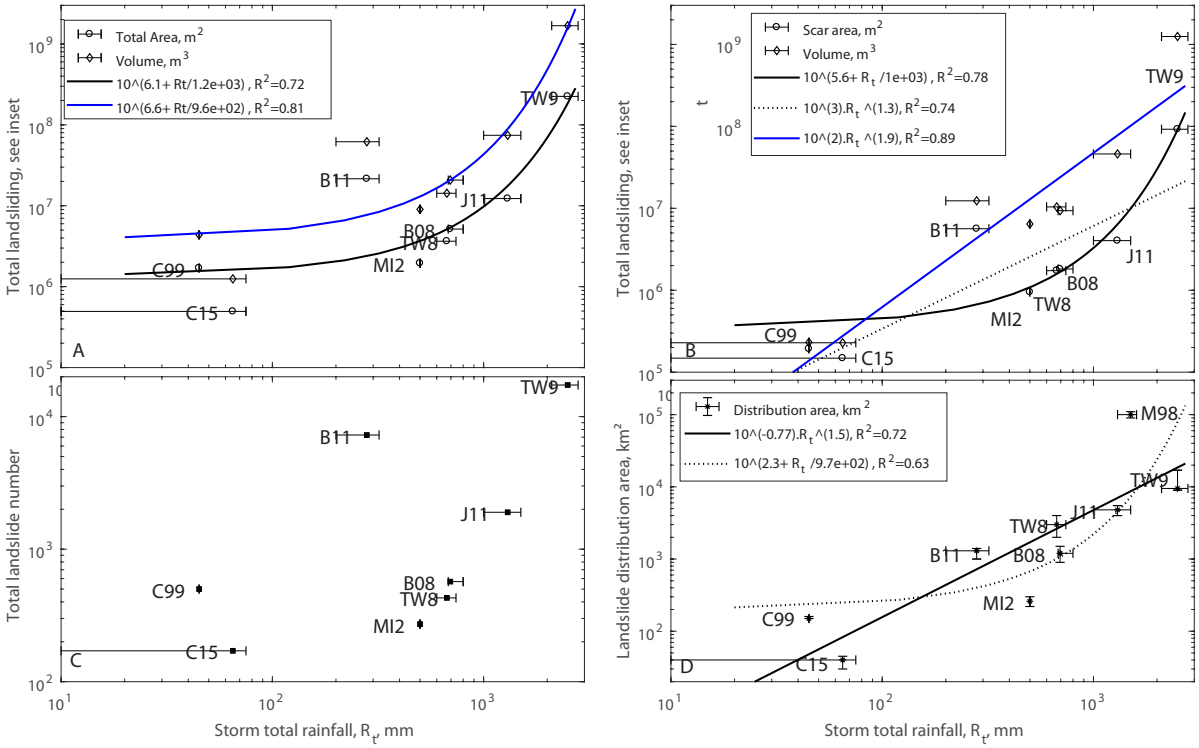

Figure 5. Total landsliding in area and volume derived from whole landslides (A) or from scar estimates only (B), total landslide number (C) and landslide distribution area (D) against storm total rainfall. M98 is for Mitch 1998. Horizontal error bars show a range of maximum storm rainfall when available (cf, Table 1). In A and B 1σ uncertainty on the total volumes and areas, ignoring potential landslide mis-detection (cf. methods), are smaller than the symbols ($< 10\%$). Vertical error bars are based on the range of affected areas in D, while we could not obtain quantitative uncertainties on the total number (C).

The mean landslide densities vary between $0.01 - 1\%$ and ~~$100 - 10{,}000 m^3.km^{-2}$~~ 100-10,000 $m^3.km^{-2}$ but with poor correlation with total rainfall ($R^2 = 0.01$ and $R^2 = 0.46$ for area and volume density respectively). Indeed, given that both total landsliding and distribution area increase strongly with total rainfall, their ratio is relatively independent. In contrast, the maximum landslide scar density and volume density range from 0.1 to 5% and 0.002 to 1.5 millions ~~$m^3.km^{-2}$~~ $m^3.km^{-2}$, respectively, and are strongly correlated with a power-law of total rainfall ($R^2 = 0.76$ and $R^2 = 0.95$). We found very similar correlations when computing the local density on a grid of 0.03° or 0.1°, but degraded correlations when using the whole landslide area to compute landslide density ($R^2 = 0.40$ and $R^2 = 0.69$). We also note that, as for the total landsliding, maximum landslide density and volume density are significantly correlated with peak rainfall intensity, $I3$ ($R^2 = 0.58$ and $R^2 = 0.67$, respectively), and duration, D ($R^2 = 0.70$ and $R^2 = 0.73$, respectively), although less strongly than with total rainfall.

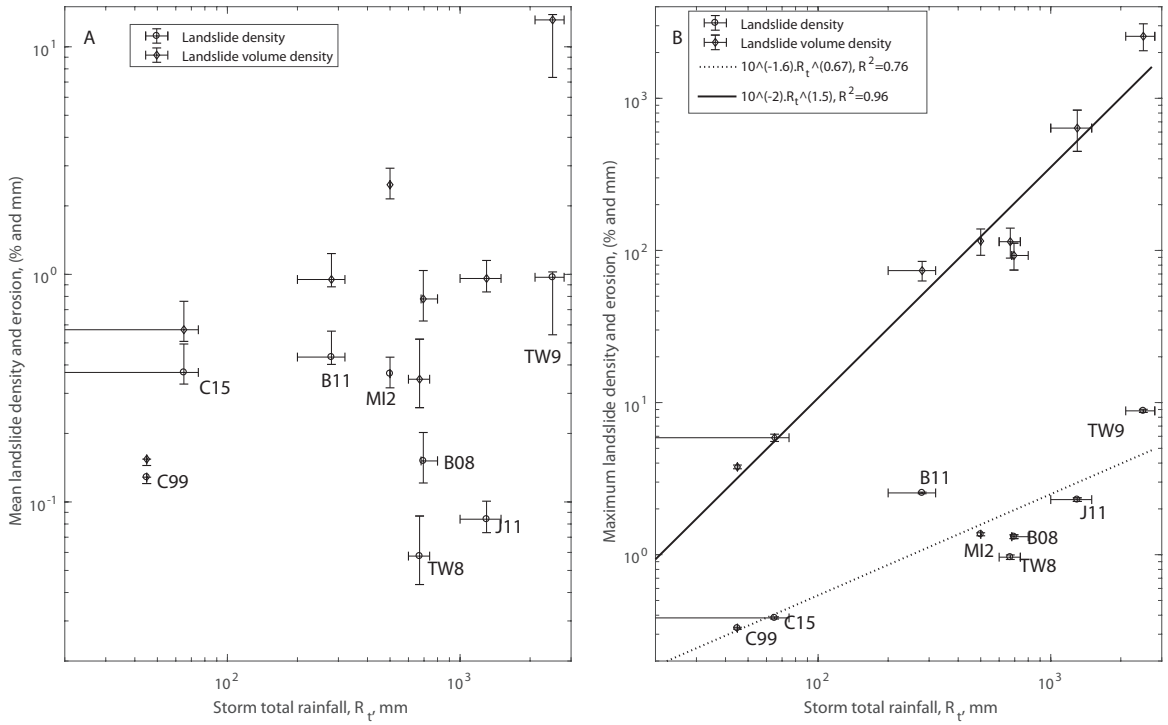

Figure 6. Mean landslide density (A) and peak landslide density in a 0.05° sliding window (B), against storm total rainfall. Landslide area and volume are derived from scar estimates, i.e., removing runout contribution. Horizontal error bars shows a range of maximum storm rainfall when available (cf, Table 1). Vertical error bars are based on the range of affected area in A (the most uncertain term), and represents 1σ uncertainty on the total volume and area density in B, ignoring potential landslide mis-detection (cf. methods).

3.2.3 Landslide size, runout and position on slope

The ~~power-law~~ decay exponents of the distribution of landslide ~~size or~~ area do not correlate significantly with any storm metrics (Intensity, duration or total rainfall) ($|R| < 0.1$). However, after runout normalization, the decay exponents of landslide scar area correlate with all metrics, although with significant scatter ($R^2 \sim 0.5$ Fig 3, 7). The two largest storms (J11 and TW9) have the lowest exponents ($\alpha + 1 \sim 1.8$), and thus a large proportion of very large landslides, while the two smallest storms (C15 and C99) have a small proportion of large landslides and large exponents ($\alpha + 1 \sim 2.7$). However, intermediate cases are very scattered, as B11 and TW8 have similar total rainfall, peak intensity and duration but very different distribution with $\alpha + 1 = 1.9$ and with $\alpha + 1 = 2.6$, respectively. Still, randomly removing one event (i.e., jackknife sampling) we obtained R^2 between 0.4 and 0.7, with a similar mean R^2 about 0.5.

The decay exponents of the equivalent aspect ratio (Fig 3, ~~S??~~Suppl. 6) do not correlate significantly with any storm metrics (Intensity, duration or total rainfall) ($|R| < 0.2$). Indeed, long runout landslides are abundant for the smallest storm, C99 and C15, as well as for the second largest storm, J11, but are ~~less frequent for the~~ relatively rare for other storms (e.g., MI2,TW8,

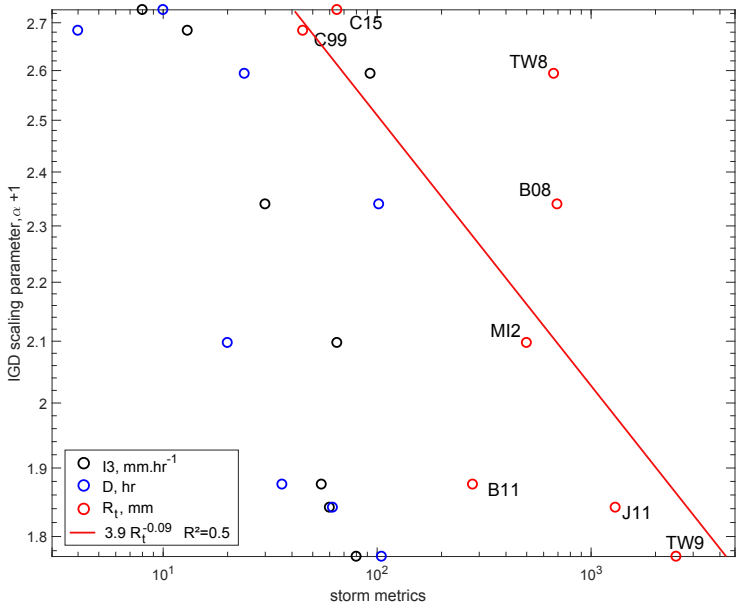

Figure 7. Landslide scar size distribution decay exponents against storm total rainfall (red), storm duration (blue) and storm peak intensity (black). The best least-squares fit is shown in red. The reduction of the decay exponents with increasing storm magnitude indicates an increase in the proportion of large landslides relative to small landslide.

B08), spanning the whole range of storm indexes. Similarly, the mean or modal aspect ratio are similar for all event across all storm metrics, except for C99 which is heavily dominated by debris flow and has a modal aspect ratio > 10.

~~However, we note that the events where landslides occurred preferentially on steep slopes correspond to very short duration rainfall events (~~We have observed that almost the eight events behave similarly with respect to the distribution of topographic slopes, not suggesting strong link with the individual storms properties. The C99 ~~and~~ event has a different behavior that may relate to the fact that it was the shortest storm with the smallest total, or that it was the only cases occurring in high elevation terrain, with sparse vegetation. C15~~), while the events with the strongest undersampling of steep slopesare the longest storms (B08). Indeed, if we compute the mean landslide/topography sampling ratio between 10 and 30°~~, the second shortest and smallest storm event may also have strong oversampling about 20°~~above the local topographic mode, we find a correlation of this index with storm duration. A power-law fit is most appropriate and explains ~ 70% of the variance (Fig **??**). This correlation may even be underestimated considering that the Brazil 2008 storm, occurred after several weeks of anomalously elevated rainfall, suggesting a longer duration.~~ beyond S_M but the limited number of landslides does not allow to confirm the significance of this oversampling.

4 Discussion

4.1 Scaling between rainfall and landsliding

We found that total landsliding, peak landslide density and the distribution area of landsliding were all best described as increasing as a power-law or exponential function of the total storm rainfall, R_t. Our mechanistic understanding of landsliding predicts that, for a given site, the driving force leading to failure is the reduction of normal load and friction due to the increasing ~~pore water~~ pore-water pressure (Iverson, 2000). This requires progressive saturation of the material above the failure plane, and depends directly on the total amount of water poured on the slopes. However, we can envision that landscapes may rapidly reach an equilibrium in which all unstable slopes under rainfall conditions frequently occurring would have been removed. In this framework, the rainfall amount relative to the local climate would be more relevant than absolute rainfall, requiring an analysis in terms of deviation from the mean rainfall or in terms of rainfall percentiles (e.g., Guzzetti 2007). Although we could not define rainfall percentiles in each area, we note that normalizing R_t by the mean monthly rainfall relevant for each storm, we still find a decent correlation with the peak landslide density, implying climate normalized rainfall variable may be driving landsliding (Fig Suppl. 8). The antecedent rainfall is also expected to play a key role, in controlling the saturation level before the triggering storm (e.g., Gabet et al., 2004; Godt et al., 2006). However, if the regolith is already close to the field capacity, significant parts of antecedent rainfall may be drained from the regolith within some hours or days (Wilson and Wieczorek, 1995), and as result, the contribution of past storms may be negligible compared to heavy rainfalls over relatively short time intervals (1-4 days). However, for moderate storms, like C15 or C99, and especially during dry periods when the slope is saturated below field capacity, the role of antecedent rainfall may be more substantial. Thus, we expect that moderate storms happening after prolonged dry or wet periods may deviate downward or upward from the scaling, respectively. We also note that an abundance of larger and deeper landslide strongly influencing the total volume or erosion, may depend on deeper water level rather than regolith saturation and thus may be most sensitive to water accumulation over several days rather than a few hours (Van Asch et al., 1999; Uchida et al., 2013). Therefore, although we obtained a good correlation without considering antecedent rainfall, its role should be assessed in future refined scalings. Last, the scaling reported here is based on events where all landslides occurred within a short time frame (few hours to few days), and would not apply to a monsoon setting where landslides occur more or less continuously during several weeks (Gabet et al., 2004; Dahal and Hasegawa, 2008), driven by continuous, heavy but unexceptional, rainfall. Indeed, in a long period with fluctuating rainfall such as the monsoon, drainage and storage of water will certainly not be negligible and the derivation of a soil water content proxy will be necessary (e.g., Gabet et al., 2004) .

The strong correlation between R_t and ~~distribution area~~ A_d, suggests that storms able to generate greater amounts of rainfall also tends to deliver a sufficient amount of rain over broader areas. ~~We have no clear physical explanation of why this could be the case.~~ For tropical storms and hurricanes (5 out 9 cases in Fig 5D) a number of studies (cf., Jiang et al., 2008, and references therein) , found that the maximum inland storm total rainfall (i.e, R_t for us) correlated well ($R > 0.7$) with a rainfall potential defined as the product of storm diameter and storm mean rainfall rate within this diameter over storm velocity, each terms measured 1-3 days before the storm made landfall. It was also generally observed that rainfall intensity is higher closer of the storm core, thus

potentially tightening the link between R_t and a given storm radius with intense rainfall and high landslide probability. These observations would imply linear proportionality between R_t and A_d and could be consistent with the observed power-law trend (exponent 1.5) (Fig 5), especially if some further links between R_t and mean storm intensity or velocity exist. Potential links between R_t and A_d for smaller scale storms (C99,C15, B08 and B11) are harder to interpret, and we cannot exclude that it is a coincidence allowed by our small number of events. In any case the broader zone is not likely to receive homogeneous rainfall amount, decoupling mean landslide density from storm maximum strength (Fig 6A). The variability of rainfall within these extended zones is likely a main control on the spatial variability of landslide density, although lithological properties or slope distribution may also matter. Indeed lithological boundaries, or a lack of steep slopes can sometimes explain spatial variability in landsliding, but not all of it (e.g., Fig Suppl. ~~6~~9). In any case, it seems clear that to predict the spatial variability of landsliding, the rainfall spatio-temporal pattern is a ~~prime~~ primary requirement. The good correlation between storm total rainfall and peak landslide density ~~,~~ is encouraging and suggests that, as most mountainous regions may have sparse instrumental coverage, the use of satellite measurements (Ushio et al., 2009; Huffman et al., 2007) or meso-scale meteorological models (e.g., Lafore et al., 1997) may be required to understand the spatial pattern of rainfall induced landsliding.

A few non-linear scaling between total landsliding and total rainfall have been reported at the catchment scale, but were derived from datasets not easily comparable to the one presented in this study (Reid, 1998; Chen et al., 2013; Marc et al., 2015). The details of this scaling is of importance in order to understand the impact of extreme rainfall events and more generally which type of rainfall event contributes most to sediment transfer over long time scales (Reid and Page, 2003; Chen et al., 2015). We also found non-linear scaling between R_t and total landslide area, but without a strong statistical difference between exponential or power-law. Exponential functions yield a minimum landsliding amount at low rainfall, that is not physical justified. This apparent contradiction may, however, be resolved by considering a rainfall threshold below which landsliding is null. The higher correlation between R_t and total volume, is likely due to the fact that R_t correlates very well with maximum landslide size ($R^2 = 0.8$ with whole landslides, $R^2 = 0.9$ and almost linear correlation with scar estimates, Figure Suppl ~~5~~10), with large landslides contributing most of the total volume and erosion. A correlation between R_t and large landsliding may arise because landslide stability is determined by the ratio between pore pressure and the total normal stress on the slip plane, meaning that larger landslides that have usually deeper failure planes (Larsen et al., 2010), may only fail with greater precipitation amount. However, given that ~~we do not observe a clear~~ the trend between total rainfall and ~~size distribution, a competing hypothesis may be that this correlation is just~~ the landslide size distribution is much weaker, this correlation may also partly result from a sampling bias as the probability to draw large landslides increases with the total number of landslides. For now, our unreliable estimates of total landslide number do not allow to ~~test this alternative~~quantify this effect.

~~The scaling with rainfall may also~~ In any case, several caveat should be taken with the preliminary scaling between total storm rainfall and total landsliding. First, the definition and limit of a single "storm" is not generally agreed in the meteorological community, because the atmospheric fluids suffer perturbations with scale interactions, and therefore with events not independent from each other. Ideally, future studies could categorize storms according to some space-time filtering and analyze the scaling with total landsliding for each storm category. Currently, our database is not sufficient for this. Second, linking total rainfall in a limited area and the total landsliding within the storm footprint implicitly suggests that storm rainfall is somewhat structured

with some internal correlations between peak rainfall, storm size, and the spatial pattern of rainfall intensity within the storm. This seems to be the case for large tropical storms (Jiang et al., 2008) , but should be explored for a broader range of storm types. Orographic effects (e.g., Houze, 2012; Taniguchi et al., 2013) , focussing high intensity rainfall on topographic barriers, may also enhance such correlation between local total rainfall, and the broader pattern of rainfall and landsliding. Last, the scaling with rainfall may also be obscured by outliers due to processes not controlled by rainfall. For example, the inclusion of the very long runout components in several inventories led to larger scattering for both power-law and exponential models and to favor the latter. Therefore, the proposed runout correction seem essential for future studies. Another issue concerns the normalization of landscape parameters affecting the susceptibility to landsliding, such as hillslope steepness and mechanical strength (Schmidt and Montgomery, 1995; Parise and Jibson, 2000; Marc et al., 2016). ~~The impact of hillslope steepness may be difficult to include as it seems to vary with the type of storms (Fig **??**), as discussed below.~~ Nevertheless, the proportion of flat or submerged land within the area of the most intense rainfall must limit the total landsliding, as it was certainly the case for MI2 or B08 (Fig 1). Recent, widespread antecedent landsliding may also reduce subsequent susceptibility to rainfall triggering by removing the weak layer of soil or regolith on steep slopes. In the pre-event imagery we did not see specific evidence of such limitation, except maybe for J11, where abundant pre-event fresh landsliding were visible near 136,25°E/34,29°N and 135,9°E/34,20° and very few new landslides occurred. More systematic evaluation of this effect may be important when comparing quantitatively landslide and rainfall pattern. In any case, it is clear that further analysis of this database, possibly extended with additional landslide inventories, should be used by future studies to refine the scaling with rainfall and incorporate the effects of controlling parameters such as available topography, antecedent rainfall or regolith properties (e.g., strength and permeability).

4.2 Relation between rainfall and landslide properties

We ~~do not find a clear influence of storm metrics on landslide scar areas nor runout areas distributions. This does not necessarily imply that storm properties do not affect landslide runout or scar size, but suggest that this effect is minor compared to other factors varying~~ found an increase in the proportion of large landslide scars with all storm metrics, but clearest with the total rainstorm (Fig 7). This is consistent with the idea that large landslides require larger amount of rainfall to be triggered (Van Asch et al., 1999) , as discussed above and exemplified with the strong correlation between R_t and maximal landslide scar (Fig Suppl. 10). The large remaining scatter suggests that other differences between the inventories ~~. For example~~matter, such as differences in the mechanical properties of the substrate (e.g., Stark and Guzzetti, 2009) . Indeed, large lithological contrast exist between each events, and sometimes within event (~~J11, TW9,~~ Fig Suppl. ~~6).~~ 9). The variability in extent and thickness of weak superficial layers (i.e., soils) between the different landscapes affected may also be important. Variations in slope distribution and relief are also wide between each case (Fig 1, 4) and have also been reported to influence landslide size (Frattini and Crosta, 2013)~~since long and steep slopes amplify runout. Therefore, it is likely that only some adequate normalization of these contributions could reveal the influence of rainfall on landslide size. Given that topography and lithology change within the landslide distribution area, accurate comparison would also require to assess the spatial variations of rainfall over these zones. Last, the relative proportion of shallow and deep landslides (i.e., small and large) must depend on the ratio of rain intensity~~

~~over regolith hydrological properties (Iverson, 2000) , allowing or impeding~~ . We note that the correlation between peak rainfall intensity is opposed to what could be expected, as more small landslide are expected for pulses of very intense rain leading to the occurrence of transient ~~water accumulation~~ high pore-water pressure pulses at shallow depth (Iverson, 2000) . Given that water retention and hydraulic conductivity may easily change by orders of magnitude between different environments, ~~focusing on rainfall intensity only is likely insufficient. Thus, either conductivity~~ it may be needed to normalize intensity by the regolith hydraulic conductivity (Iverson, 2000) to understand its potential influence. For the moment we consider that the correlation between D and $I3$ and the landslide size distribution exponents likely arises because of the correlation between thes storm metrics and R_t (Fig Suppl. 4) In any case, our results suggest that it is not only the landscape properties that set the landslide size distribution, but also the trigger characteristics, as previously reported for earthquake induced landslide size distributions (Marc et al., 2016) . This means, for example, that the influence of forcing variability should be assessed ~~at first order or we should~~ and normalized before inverting landslide size distribution parameters to obtain regional variations of mechanical properties (e.g., Gallen et al., 2015) . In contrast, aspect ratio or runout did not correlate well with storm metrics and thus obscured any direct correlation between storm metrics and the decay exponents of whole landslide area. This underlines again the importance to isolate scar geometry to deconvolve processes driving landslide initiation and landslide runout. As for the landslide size distribution, landslide runout may likely be influenced by slope and relief distribution, as well as by hydrologic processes. The case of C99, with exceptional runout for most of its landslides is interpreted has the effect of a low infiltration rates favoring large runoff generation (Godt and Coe, 2007) . This may also explain the abundance of debris flow in other places (C15, J11) but cannot be verified without information on infiltration rate in these places to normalize the intensity variations. An alternative could be to study various storms occurring over the same region, and where infiltration rate or conductivity could be assumed constant, for example with datasets from multiple typhoons in Taiwan (Chen et al., 2013).

Finally, we observed ~~at least two regimes of relations between landsliding and the topographical slopes, one in which landslides occur preferentially on the steepest part of the topography and the other in which the landslides occur almost uniformly on slopes~~ that most rainfall induced landslide inventories sample the topographic slope distribution with a minor oversampling beyond the topographic ~~mode~~ modal slope (Fig 4). ~~It is yet unclear whether the case of Brazil 2008 with a systematic under-sampling of steep slopes is another behavior or is in the continuity of the latter type. In any case, these behaviors do not correlate with the topographic mode itself or the total landsliding. We note that in the~~ This is in contrast with the case of earthquake triggered landslides, where we systematically observe preferential landsliding on the steepest slopes (Parise and Jibson, 2000; Gorum et al., 2013, 2014)(Fig 4), quite similar to ~~one end-member behavior~~the case of C99. One dimensional static force balance shows that the steepest slopes are the most unstable, and therefore the over-sampling of steep slopes must be expected if the forcing (~~pore water~~ pore-water pressure or shaking) is randomly distributed across the whole topography. To obtain equal sampling or under-sampling of steep slopes, the forcing intensity must be anti-correlated with slope gradient. Rainfall may be mostly independent of local slopes, but probably not the pore pressure rise that depends on the underground water circulation and thus topography. The pore pressure will thus depend crucially on vertical infiltration and drainage, but also on along-slope contributions. For example under moderate intensity, but long rainfall, ~~pore water~~ pore-water pressure will reach higher level in concave, downslope areas (Montgomery and Dietrich, 1994) with relatively large drainage area,

and thus lower slope gradient (Montgomery, 2001). In such view, landslide slope statistics would bear information on the type of rainfall, short and intense (relative to local permeability) for steep over-sampling, while equal sampling and under-sampling would relate to moderate and long rainfall. This framework ~~could explain the significant anti-correlation between the landslide-topography probability ratio and the storm duration~~ might explain the preferential location on steep slopes observed for the very short duration C99 and possibly C15 (Fig 4). ~~We tried to plot the slope-gradient vs drainage~~ However, the statistics of C15 are weak and C99 strong oversampling may relate mainly to specific mass movement triggered by surface runoff such as rilling and firehose (cf., Godt and Coe, 2007) . These processes also require high intensity, short duration events, but also low surficial infiltration rate leading to overland flow able to mobilize relatively loose surface materials. For other events, we analyzed the slope-gradient-drainage area relationship for topography and landslide subset ~~of various events without finding~~ and did not find clear over-sampling of high-drainage and gentle gradient ~~ares~~ areas in the landslide distribution. ~~This may suggest another explanation has to be put forward, or simply that a 30m~~ It is well possible that a 30 m DEM is not able to resolve accurately the fine-scale pattern of slope and drainage on the hillsides, where landslides occur~~. In any case, we note that it is often suggested that short and intense rainfall should produce mostly small landslides in contrast to long, moderate rainfall (Van Asch et al., 1999) , but our datasets suggest it may be easier to detect differences in the slope sampling of landslides for these storm end-members~~, but it may also suggest that the upslope drainage area is not the main explanation. For example, the subsurface drainage efficiency may also increase with slope gradient, thus making very steep areas less likely to develop large pore pressure and possibly explaining the preferential landsliding of slopes just above the modal slopes for almost all events, indepedent of rainfall properties. Hydro-mechanical modeling at the catchment scale (e.g., von Ruette et al., 2013) , applied on several of our dataset may be the only way to test between these different hypothesis. Further constraints on the ~~behavior of these end-members may~~ processes controlling rainfall-induced landslides may also be achieved through a discussion in terms of relative distance from ridge and river (cf, Meunier et al., 2008), as intense and brief storms should yield uniformly distributed landsliding, in contrast to longer, less intense storms favoring near river slides.

5 Conclusions

We present landslide inventories (comprising from a few hundreds to more than 15,000 ~~events~~polygons) associated with eight triggering rain storms from Asia, South America, and North America. We hypothesize that these datasets constitute a global database of rainfall-induced landslides, that allows studying a number of landslide metrics and their relations to rainfall and landscape properties. Indeed, although spanning a large range of landscape settings, whether in terms of topography, climate or vegetation, the magnitude of landsliding scales non-linearly with the magnitude of the storm, here quantified with estimates of the total rainfall. We also found that correlation between landsliding and rainfall is higher when considering landslide scar estimates obtained through a normalization of landslide runout, as the runout distribution does not clearly correlate to rainfall. Therefore, after removing the runout contribution (i.e., focussing on scars) we also find that landslide size distribution decay exponent seems to be partly controlled by totall rainfall, with a greater proportion of large landslides for larger total precipitation. This implies that variations of landslide size distribution cannot be directly interpreted as variations in landscape

properties. For total landsliding and maximum local landslide density, power-law scaling based on total rainfall explains 74% (87% for total volume) and 76% (95% for volume density) of the variance, respectively. Adding a number of other storm events as well as integrating other rainfall forcing parameters or landscape susceptibility properties have therefore the potential to yield robust prediction on the magnitude of rainfall induced landsliding. Last, we identify that ~~short storm tends to trigger landslides on the steepest slopes of the landscapes while landslides induced by long storms sample equally the~~ compared to earthquakes, storms tend to trigger landslides that only slightly oversample the topographic slope distribution, possibly ~~relating to~~ due to faster drainage on steep slopes or to underground water accumulation on high drainage-low gradient portions of the hillslope. This may bring new, although less straightforward, implications for the difference in resulting topography of bedrock landscape dominated by rainfall-induced or earthquake-induced landslides (Densmore and Hovius, 2000). Although preliminary these insights and scaling clearly show the value of ~~collecting comprehensive landslide inventories~~ mapping systematically a large sample of the landslides that can be related to a single storm and we identified a number of recent storm events were such type of inventory could be produced. Although not systematically addressed here, landslide density spatial pattern is likely strongly related to the spatio-temporal pattern of rainfall, and constraining the quantitative links between the two is another challenge that may be addressed with some of the inventories presented here. More generally, the database presented here may also serve as a benchmark for developing and comparing rainfall induced landslide models, whether empirical, semi- or fully-deterministic. These future developments are important challenges in order to understand the natural hazards posed by rainfall-induced landslides as well as their specific implication for the erosion and topographic evolution of landscapes in different climatic settings.

Acknowledgements. The authors are grateful to the thorough and constructive reviews from Dave Milledge and an anonymous reviewers that helped to improved and clarify considerably this manuscript. OM thanks Patrick Meunier for discussions on prediction interval and the statistical significance of probability distribution ratios. This work was carried with the support of the French Space Agency (CNES) through the project STREAM-LINE GLIDERS "SaTellite-based Rainfall Measurement and LandslIde detectioN for Global LandslIDE-Rainfall Scaling". Additional support by the Open Partial Agreement "Major Hazards" of Council of Europe through the project "Space data in Disaster Risk Reduction: using satellite precipitation data and hydrological information for leapfrogging landslide forecasting" was available.

Data availability. All imagery used to map the landslides is available in public repository except the images from Formosat-2, Geoeye-1 and airphotos used for the events in Colorado, Micronesia and Japan. For the two former, landslide maps are directly available from the USGS at http://pubs.usgs.gov/of/2003/ofr-03-050/ and https://pubs.usgs.gov/of/2004/1348/. For Japan and Brazil, extensive high resolution imagery is available over most of the areas of interest in Google Earth. The new digitized landslide inventories are available upon request.

The authors acknowledge support from the Typhoon and Flood Research Institute, National and Applied Research Laboratories which provide rain gage information in Taiwan from the Data Bank for Atmospheric and Hydrologic Research service (https://dbahr.narlabs.org.tw).

In Japan, rain gage data was accessed thanks to Japan Meteorological Agency. The authors gratefully used the global GSMaP rainfall products (http://sharaku.eorc.jaxa.jp/GSMaP_crest/) and SRTM-30 m DEM provided by USGS https://gdex.cr.usgs.gov/gdex/

Author contributions. OM designed the study and performed all analyses with some inputs from AS, JPM and MG. TU provided landslide and rainfall data for the J11 event. SHC provided imagery and landslide data for the TW9 event. OM wrote the manuscript with contributions from all co-authors.

Competing interests. The authors declare no conflicts of interest with the present study.

References

Ardizzone, F., Basile, G., Cardinali, M., Casagli, N., Conte, S. D., Ventisette, C. D., Fiorucci, F., Garfagnoli, F., Gigli, G., Guzzetti, F., Iovine, G., Mondini, A. C., Moretti, S., Panebianco, M., Raspini, F., Reichenbach, P., Rossi, M., Tanteri, L., and Terranova, O.: Landslide inventory map for the Briga and the Giampilieri catchments, NE Sicily, Italy, Journal of Maps, 8, 176–180, https://doi.org/10.1080/17445647.2012.694271, https://doi.org/10.1080/17445647.2012.694271, 2012.

Arnone, E., Noto, L. V., Lepore, C., and Bras, R. L.: Physically-based and distributed approach to analyze rainfall-triggered landslides at watershed scale, Geomorphology, 133, 121–131, https://doi.org/10.1016/j.geomorph.2011.03.019, http://www.sciencedirect.com/science/article/pii/S0169555X11002637, 2011.

Baum, R. L., Godt, J. W., and Savage, W. Z.: Estimating the timing and location of shallow rainfall-induced landslides using a model for transient, unsaturated infiltration, Journal of Geophysical Research: Earth Surface, 115, F03 013, https://doi.org/10.1029/2009JF001321, http://onlinelibrary.wiley.com/doi/10.1029/2009JF001321/abstract, 2010.

Blodgett, T. A. and Isacks, B. L.: Landslide Erosion Rate in the Eastern Cordillera of Northern Bolivia, Earth Interactions, 11, 1–30, https://doi.org/10.1175/2007EI222.1, http://journals.ametsoc.org/doi/full/10.1175/2007EI222.1, 2007.

Bucknam, R. C., Coe, J. A., Chavarria, M. M., Godt, J. W., Tarr, A. C., Bradley, L.-A., Rafferty, S. A., Hancock, D., Dart, R. L., and Johnson, M. L.: Landslides triggered by Hurricane Mitch in Guatemala – inventory and discussion, USGS Numbered Series 2001-443, http://pubs.er.usgs.gov/publication/ofr01443, 2001.

Caine, N.: The Rainfall Intensity: Duration Control of Shallow Landslides and Debris Flows, Geografiska Annaler. Series A, Physical Geography, 62, 23–27, https://doi.org/10.2307/520449, http://www.jstor.org/stable/520449, 1980.

Camargo, L. P.: Análise integrada no meio físico dos ribeirões Braço Serafim e Máximo com ênfase nas áreas de fragilidade estrutural, Luís Alves, (SC), PhD thesis, Universidade Federal de Santa Catarina, Florianopolis, https://repositorio.ufsc.br/handle/123456789/157291, 2015.

Cannon, S. H., Haller, K. M., Ekstrom, I., Schweig, E. S., Devoli, G., Moore, D. W., Rafferty, S. A., and Tarr, A. C.: Landslide response to Hurricane Mitch rainfall in seven study areas in Nicaragua, USGS Numbered Series 2001-412-A, http://pubs.er.usgs.gov/publication/ofr01412A, 2001.

Cardinali, M., Galli, M., Guzzetti, F., Ardizzone, F., Reichenbach, P., and Bartoccini, P.: Rainfall induced landslides in December 2004 in south-western Umbria, central Italy: types, extent, damage and risk assessment, Nat. Hazards Earth Syst. Sci., 6, 237–260, https://doi.org/10.5194/nhess-6-237-2006, http://www.nat-hazards-earth-syst-sci.net/6/237/2006/, 2006.

Chang, K.-t., Chiang, S.-h., Chen, Y.-c., and Mondini, A. C.: Modeling the spatial occurrence of shallow landslides triggered by typhoons, Geomorphology, 208, 137–148, https://doi.org/10.1016/j.geomorph.2013.11.020, http://www.sciencedirect.com/science/article/pii/S0169555X13005990, 2014.

Chen, Y.-C., Chang, K.-t., Chiu, Y.-J., Lau, S.-M., and Lee, H.-Y.: Quantifying rainfall controls on catchment-scale landslide erosion in Taiwan, Earth Surface Processes and Landforms, 38, 372–382, https://doi.org/10.1002/esp.3284, http://onlinelibrary.wiley.com/doi/10.1002/esp.3284/abstract, 2013.

Chen, Y.-c., Chang, K.-t., Lee, H.-y., and Chiang, S.-h.: Average landslide erosion rate at the watershed scale in southern Taiwan estimated from magnitude and frequency of rainfall, Geomorphology, 228, 756–764, https://doi.org/10.1016/j.geomorph.2014.07.022, http://www.sciencedirect.com/science/article/pii/S0169555X14003869, 2015.

Clark, K. E., West, A. J., Hilton, R. G., Asner, G. P., Quesada, C. A., Silman, M. R., Saatchi, S. S., Farfan-Rios, W., Martin, R. E., Horwath, A. B., Halladay, K., New, M., and Malhi, Y.: Storm-triggered landslides in the Peruvian Andes and implications for topography, carbon cycles, and biodiversity, Earth Surface Dynamics, 4, 47–70, https://doi.org/10.5194/esurf-4-47-2016, http://www.earth-surf-dynam.net/4/47/2016/, 2016.

Crone, A. J., Baum, R. L., Lidke, D. J., Sather, D. N., Bradley, L.-A., and Tarr, A. C.: Landslides induced by Hurricane Mitch in El Salvador – an inventory and descriptions of selected features, USGS Numbered Series 2001-444, http://pubs.er.usgs.gov/publication/ofr01444, 2001.

Dahal, R. K. and Hasegawa, S.: Representative rainfall thresholds for landslides in the Nepal Himalaya, Geomorphology, 100, 429–443, https://doi.org/10.1016/j.geomorph.2008.01.014, http://www.sciencedirect.com/science/article/pii/S0169555X08000172, 2008.

Densmore, A. L. and Hovius, N.: Topographic fingerprints of bedrock landslides, Geology, 28, 371–374, https://doi.org/10.1130/0091-7613(2000)28<371:TFOBL>;2.0.CO;2, http://geology.geoscienceworld.org/content/28/4/371, 2000.

Domej, G., Bourdeau, C., and Lenti, L.: Mean Landslide Geometries Inferred from a Global Database of Earthquake- and Non-Earthquake-Triggered Landslides, Italian Journal of Engineering Geology and Environment, pp. 87–107, https://doi.org/10.4408/IJEGE.2017-02.O-05, http://www.ijege.uniroma1.it/rivista/ijege-17/ijege-17-volume-02/mean-landslide-geometries-inferred-from-a-global-database-of-earthquake-and-non-earthquake-triggered-landslides/ijege-17_02-domej-et-alii.pdf, 2017.

Frattini, P. and Crosta, G. B.: The role of material properties and landscape morphology on landslide size distributions, Earth and Planetary Science Letters, 361, 310–319, https://doi.org/10.1016/j.epsl.2012.10.029, http://www.sciencedirect.com/science/article/pii/S0012821X12005985, 2013.

Gabet, E. J., Burbank, D. W., Putkonen, J. K., Pratt-Sitaula, B. A., and Ojha, T.: Rainfall thresholds for landsliding in the Himalayas of Nepal, Geomorphology, 63, 131–143, https://doi.org/10.1016/j.geomorph.2004.03.011, http://www.sciencedirect.com/science/article/pii/S0169555X04001114, 2004.

Gallen, S. F., Clark, M. K., and Godt, J. W.: Coseismic landslides reveal near-surface rock strength in a high-relief, tectonically active setting, Geology, 43, 11–14, https://doi.org/10.1130/G36080.1, http://geology.geoscienceworld.org/content/43/1/11, 2015.

Gariano, S. L. and Guzzetti, F.: Landslides in a changing climate, Earth-Science Reviews, 162, 227–252, https://doi.org/10.1016/j.earscirev.2016.08.011, http://www.sciencedirect.com/science/article/pii/S0012825216302458, 2016.

Godt, J. W. and Coe, J. A.: Alpine debris flows triggered by a 28 July 1999 thunderstorm in the central Front Range, Colorado, Geomorphology, 84, 80–97, https://doi.org/10.1016/j.geomorph.2006.07.009, http://www.sciencedirect.com/science/article/pii/S0169555X06002868, 2007.

Godt, J. W., Baum, R. L., and Chleborad, A. F.: Rainfall characteristics for shallow landsliding in Seattle, Washington, USA, Earth Surface Processes and Landforms, 31, 97–110, https://doi.org/10.1002/esp.1237, http://onlinelibrary.wiley.com/doi/10.1002/esp.1237/abstract, 2006.

Gorum, T., van Westen, C. J., Korup, O., van der Meijde, M., Fan, X., and van der Meer, F. D.: Complex rupture mechanism and topography control symmetry of mass-wasting pattern, 2010 Haiti earthquake, Geomorphology, 184, 127–138, https://doi.org/10.1016/j.geomorph.2012.11.027, http://www.sciencedirect.com/science/article/pii/S0169555X12005478, 2013.

Gorum, T., Korup, O., van Westen, C. J., van der Meijde, M., Xu, C., and van der Meer, F. D.: Why so few? Landslides triggered by the 2002 Denali earthquake, Alaska, Quaternary Science Reviews, 95, 80–94, https://doi.org/10.1016/j.quascirev.2014.04.032, http://www.sciencedirect.com/science/article/pii/S0277379114001632, 2014.

Guzzetti, F., Cardinali, M., Reichenbach, P., Cipolla, F., Sebastiani, C., Galli, M., and Salvati, P.: Landslides triggered by the 23 November 2000 rainfall event in the Imperia Province, Western Liguria, Italy, Engineering Geology, 73, 229–245, https://doi.org/10.1016/j.enggeo.2004.01.006, http://www.sciencedirect.com/science/article/pii/S0013795204000225, 2004.

Guzzetti, F., Peruccacci, S., Rossi, M., and Stark, C. P.: The rainfall intensity–duration control of shallow landslides and debris flows: an update, Landslides, 5, 3–17, https://doi.org/10.1007/s10346-007-0112-1, http://link.springer.com/article/10.1007/s10346-007-0112-1, 2008.

Harp, E. and Jibson, R.: Landslides triggered by the 1994 Northridge, California, earthquake, Bulletin of the Seismological Society of America, 86, S319–S332, 1996.

Harp, E. L., Hagaman, K. W., Held, M. D., and McKenna, J. P.: Digital inventory of landslides and related deposits in Honduras triggered by Hurricane Mitch, USGS Numbered Series 2002-61, U.S. Geological Survey, Reston, VA, http://pubs.er.usgs.gov/publication/ofr0261, 2002.

Harp, E. L., Reid, M. E., and Michael, J. A.: Hazard analysis of landslides triggered by Typhoon Chata'an on July 2, 2002, in Chuuk State, Federated States of Micronesia, USGS Numbered Series 2004-1348, http://pubs.er.usgs.gov/publication/ofr20041348, 2004.

Houze, R. A.: Orographic effects on precipitating clouds, Reviews of Geophysics, 50, https://doi.org/10.1029/2011RG000365, https://agupubs.onlinelibrary.wiley.com/doi/abs/10.1029/2011RG000365, 2012.

Hovius, N., Stark, C. P., and Allen, P. A.: Sediment flux from a mountain belt derived by landslide mapping, Geology, 25, 231–234, https://doi.org/10.1130/0091-7613(1997)025<0231:SFFAMB>2.3.CO;2, http://geology.geoscienceworld.org/content/25/3/231, 1997.

Huffman, G. J., Bolvin, D. T., Nelkin, E. J., Wolff, D. B., Adler, R. F., Gu, G., Hong, Y., Bowman, K. P., and Stocker, E. F.: The TRMM Multisatellite Precipitation Analysis (TMPA): Quasi-Global, Multiyear, Combined-Sensor Precipitation Estimates at Fine Scales, Journal of Hydrometeorology, 8, 38–55, https://doi.org/10.1175/JHM560.1, https://journals.ametsoc.org/doi/abs/10.1175/JHM560.1, 2007.

Iverson, R. M.: Landslide triggering by rain infiltration, Water Resources Research, 36, 1897–1910, https://doi.org/10.1029/2000WR900090, http://onlinelibrary.wiley.com/doi/10.1029/2000WR900090/abstract, 2000.

Jiang, H., Halverson, J. B., Simpson, J., and Zipser, E. J.: Hurricane "Rainfall Potential" Derived from Satellite Observations Aids Overland Rainfall Prediction, Journal of Applied Meteorology and Climatology, 47, 944–959, https://doi.org/10.1175/2007JAMC1619.1, https://journals.ametsoc.org/doi/abs/10.1175/2007JAMC1619.1, 2008.

Jibson, R. W., Prentice, C. S., Borissoff, B. A., Rogozhin, E. A., and Langer, C. J.: Some observations of landslides triggered by the 29 April 1991 Racha earthquake, Republic of Georgia, Bulletin of the Seismological Society of America, 84, 963–973, http://bssa.geoscienceworld.org/content/84/4/963, 1994.

Jibson, R. W., Harp, E. L., and Michael, J. A.: A method for producing digital probabilistic seismic landslide hazard maps, Engineering Geology, 58, 271–289, https://doi.org/10.1016/S0013-7952(00)00039-9, http://www.sciencedirect.com/science/article/pii/S0013795200000399, 2000.

Katz, O., Morgan, J. K., Aharonov, E., and Dugan, B.: Controls on the size and geometry of landslides: Insights from discrete element numerical simulations, Geomorphology, 220, 104–113, https://doi.org/10.1016/j.geomorph.2014.05.021, http://www.sciencedirect.com/science/article/pii/S0169555X1400289X, 2014.

Keefer, D. K., Wilson, R. C., Mark, R. K., Brabb, E. E., Brown, W. M., Ellen, S. D., Harp, E. L., Wieczorek, G. F., Alger, C. S., and Zatkin, R. S.: Real-Time Landslide Warning During Heavy Rainfall, Science, 238, 921–925, https://doi.org/10.1126/science.238.4829.921, http://science.sciencemag.org/content/238/4829/921, 1987.

Kirschbaum, D., Adler, R., Adler, D., Peters-Lidard, C., and Huffman, G.: Global Distribution of Extreme Precipitation and High-Impact Landslides in 2010 Relative to Previous Years, Journal of Hydrometeorology, 13, 1536–1551, https://doi.org/10.1175/JHM-D-12-02.1, http://journals.ametsoc.org/doi/abs/10.1175/JHM-D-12-02.1, 2012.

Kirschbaum, D. B., Adler, R., Hong, Y., Hill, S., and Lerner-Lam, A.: A global landslide catalog for hazard applications: method, results, and limitations, Natural Hazards, 52, 561–575, https://doi.org/10.1007/s11069-009-9401-4, http://link.springer.com/article/10.1007/s11069-009-9401-4, 2009.

Kubota, T., Shige, S., Hashizume, H., Ushio, T., Aonashi, K., Kachi, M., and Okamoto, K.: Global Precipitation Map using Satelliteborne Microwave Radiometers by the GSMaP Project : Production and Validation, in: 2006 IEEE MicroRad, pp. 290–295, https://doi.org/10.1109/MICRAD.2006.1677106, 2006.

Lafore, J. P., Stein, J., Asencio, N., Bougeault, P., Ducrocq, V., Duron, J., Fischer, C., Héreil, P., Mascart, P., Masson, V., Pinty, J. P., Redelsperger, J. L., Richard, E., and Arellano, J. V.-G. d.: The Meso-NH Atmospheric Simulation System. Part I: adiabatic formulation and control simulations, Annales Geophysicae, 16, 90–109, https://doi.org/10.1007/s00585-997-0090-6, https://link.springer.com/article/10.1007/s00585-997-0090-6, 1997.

Larsen, I., Montgomery, D., and Korup, O.: Landslide erosion controlled by hillslope material, Nature Geoscience, 3, 247–251, 2010.

Lehmann, P. and Or, D.: Hydromechanical triggering of landslides: From progressive local failures to mass release, Water Resources Research, 48, W03 535, https://doi.org/10.1029/2011WR010947, http://onlinelibrary.wiley.com/doi/10.1029/2011WR010947/abstract, 2012.

Liao, H.-W. and Lee, C.: Landslides triggered by Chi-Chi earthquake, in: Proceedings of the 21st Asian conference on remote sensing, vol. 1, pp. 383–388, 2000.

Malamud, B. D., Turcotte, D. L., Guzzetti, F., and Reichenbach, P.: Landslide inventories and their statistical properties, Earth Surface Processes and Landforms, 29, 687–711, https://doi.org/10.1002/esp.1064, http://onlinelibrary.wiley.com/doi/10.1002/esp.1064/abstract, 2004.

Marc, O. and Hovius, N.: Amalgamation in landslide maps: effects and automatic detection, Nat. Hazards Earth Syst. Sci., 15, 723–733, https://doi.org/10.5194/nhess-15-723-2015, http://www.nat-hazards-earth-syst-sci.net/15/723/2015/, 2015.

Marc, O., Hovius, N., Meunier, P., Uchida, T., and Hayashi, S.: Transient changes of landslide rates after earthquakes, Geology, 43, 883–886, https://doi.org/10.1130/G36961.1, http://geology.geoscienceworld.org/content/early/2015/08/21/G36961.1, 2015.

Marc, O., Hovius, N., Meunier, P., Gorum, T., and Uchida, T.: A seismologically consistent expression for the total area and volume of earthquake-triggered landsliding, Journal of Geophysical Research: Earth Surface, 121, 640–663, https://doi.org/10.1002/2015JF003732, http://onlinelibrary.wiley.com/doi/10.1002/2015JF003732/abstract, 2016.

Marc, O., Meunier, P., and Hovius, N.: Prediction of the area affected by earthquake-induced landsliding based on seismological parameters, Nat. Hazards Earth Syst. Sci., 17, 1159–1175, https://doi.org/10.5194/nhess-17-1159-2017, https://www.nat-hazards-earth-syst-sci.net/17/1159/2017/, 2017.

Meunier, P., Hovius, N., and Haines, A. J.: Regional patterns of earthquake-triggered landslides and their relation to ground motion, Geophysical Research Letters, 34, L20 408, https://doi.org/10.1029/2007GL031337, http://onlinelibrary.wiley.com/doi/10.1029/2007GL031337/abstract, 2007.

Meunier, P., Hovius, N., and Haines, J. A.: Topographic site effects and the location of earthquake induced landslides, Earth and Planetary Science Letters, 275, 221–232, https://doi.org/10.1016/j.epsl.2008.07.020, http://www.sciencedirect.com/science/article/pii/S0012821X08004536, 2008.

Meunier, P., Uchida, T., and Hovius, N.: Landslide patterns reveal the sources of large earthquakes, Earth and Planetary Science Letters, 363, 27–33, https://doi.org/10.1016/j.epsl.2012.12.018, http://www.sciencedirect.com/science/article/pii/S0012821X12007042, 2013.

Milledge, D. G., Bellugi, D., McKean, J. A., Densmore, A. L., and Dietrich, W. E.: A multidimensional stability model for predicting shallow landslide size and shape across landscapes, Journal of Geophysical Research: Earth Surface, 119, 2014JF003 135, https://doi.org/10.1002/2014JF003135, http://onlinelibrary.wiley.com/doi/10.1002/2014JF003135/abstract, 2014.

Mondini, A. C.: Measures of Spatial Autocorrelation Changes in Multitemporal SAR Images for Event Landslides Detection, Remote Sensing, 9, 554, https://doi.org/10.3390/rs9060554, http://www.mdpi.com/2072-4292/9/6/554, 2017.

Montgomery, D. R.: Slope Distributions, Threshold Hillslopes, and Steady-state Topography, American Journal of Science, 301, 432–454, https://doi.org/10.2475/ajs.301.4-5.432, http://www.ajsonline.org/content/301/4-5/432, 2001.

Montgomery, D. R. and Dietrich, W. E.: A physically based model for the topographic control on shallow landsliding, Water Resources Research, 30, 1153–1171, https://doi.org/10.1029/93WR02979, http://onlinelibrary.wiley.com/doi/10.1029/93WR02979/abstract, 1994.

Netto, A. L. C., Sato, A. M., Avelar, A. d. S., Vianna, L. G. G., Araújo, I. S., Ferreira, D. L. C., Lima, P. H., Silva, A. P. A., and Silva, R. P.: January 2011: The Extreme Landslide Disaster in Brazil, in: Landslide Science and Practice, pp. 377–384, Springer, Berlin, Heidelberg, https://link.springer.com/chapter/10.1007/978-3-642-31319-6_51, dOI: 10.1007/978-3-642-31319-6_51, 2013.

Nowicki, M. A., Wald, D. J., Hamburger, M. W., Hearne, M., and Thompson, E. M.: Development of a globally applicable model for near real-time prediction of seismically induced landslides, Engineering Geology, 173, 54–65, https://doi.org/10.1016/j.enggeo.201s4.02.002, http://www.sciencedirect.com/science/article/pii/S0013795214000301, 2014.

Ono, K., Kazama, S., and Ekkawatpanit, C.: Assessment of rainfall-induced shallow landslides in Phetchabun and Krabi provinces, Thailand, Natural Hazards, 74, 2089–2107, https://doi.org/10.1007/s11069-014-1292-3, https://link.springer.com/article/10.1007/s11069-014-1292-3, 2014.

Parise, M. and Jibson, R. W.: A seismic landslide susceptibility rating of geologic units based on analysis of characteristics of landslides triggered by the 17 January, 1994 Northridge, California earthquake, Engineering Geology, 58, 251–270, https://doi.org/10.1016/S0013-7952(00)00038-7, http://www.sciencedirect.com/science/article/pii/S0013795200000387, 2000.

Petley, D.: Global patterns of loss of life from landslides, Geology, 40, 927–930, https://doi.org/10.1130/G33217.1, http://geology.geoscienceworld.org/content/40/10/927, 2012.

Pozzobon, M.: ANÁLISE DA SUSCETIBILIDADE A DESLIZAMENTOS NO MUNICÍPIO DE BLUMENAU/SC: UMA ABORDAGEM PROBABILÍSTICA ATRAVÉS DA APLICAÇÃO DA TÉCNICA PESOS DE EVIDÊNCIA., PhD thesis, UNIVERSIDADE FEDERAL DO PARANÁ, Curitiba, http://www.floresta.ufpr.br/defesas/pdf_dr/2013/t342_0370-D.pdf, 2013.

Reid, L. M.: Calculation of average landslide frequency using climatic records, Water Resources Research, 34, 869–877, https://doi.org/10.1029/97WR02682, http://onlinelibrary.wiley.com/doi/10.1029/97WR02682/abstract, 1998.

Reid, L. M. and Page, M. J.: Magnitude and frequency of landsliding in a large New Zealand catchment, Geomorphology, 49, 71–88, https://doi.org/10.1016/S0169-555X(02)00164-2, http://www.sciencedirect.com/science/article/pii/S0169555X02001642, 2003.

Saito, H. and Matsuyama, H.: Catastrophic Landslide Disasters Triggered by Record-Breaking Rainfall in Japan: Their Accurate Detection with Normalized Soil Water Index in the Kii Peninsula for the Year 2011, Sola, 8, 81–84, https://doi.org/10.2151/sola.2012-021, 2012.

Saito, H., Korup, O., Uchida, T., Hayashi, S., and Oguchi, T.: Rainfall conditions, typhoon frequency, and contemporary landslide erosion in Japan, Geology, 42, 999–1002, https://doi.org/10.1130/G35680.1, http://geology.geoscienceworld.org/content/42/11/999, 2014.

Schmidt, K. M. and Montgomery, D. R.: Limits to Relief, Science, 270, 617–620, https://doi.org/10.1126/science.270.5236.617, http://www.sciencemag.org/content/270/5236/617, 1995.

Stark, C. P. and Guzzetti, F.: Landslide rupture and the probability distribution of mobilized debris volumes, Journal of Geophysical Research: Earth Surface, 114, F00A02, https://doi.org/10.1029/2008JF001008, http://onlinelibrary.wiley.com/doi/10.1029/2008JF001008/abstract, 2009.

Stark, C. P. and Hovius, N.: The characterization of landslide size distributions, Geophysical Research Letters, 28, 1091–1094, https://doi.org/10.1029/2000GL008527, http://onlinelibrary.wiley.com/doi/10.1029/2000GL008527/abstract, 2001.

Stumpf, A., Lachiche, N., Malet, J.-P., Kerle, N., and Puissant, A.: Active Learning in the Spatial Domain for Remote Sensing Image Classification, IEEE Transactions on Geoscience and Remote Sensing, 52, 2492–2507, https://doi.org/10.1109/TGRS.2013.2262052, 2014.

Taniguchi, A., Shige, S., Yamamoto, M. K., Mega, T., Kida, S., Kubota, T., Kachi, M., Ushio, T., and Aonashi, K.: Improvement of High-Resolution Satellite Rainfall Product for Typhoon Morakot (2009) over Taiwan, Journal of Hydrometeorology, 14, 1859–1871, https://doi.org/10.1175/JHM-D-13-047.1, http://journals.ametsoc.org/doi/full/10.1175/JHM-D-13-047.1, 2013.

Tanyaş, H., van Westen, C. J., Allstadt, K. E., Anna Nowicki Jessee, M., Görüm, T., Jibson, R. W., Godt, J. W., Sato, H. P., Schmitt, R. G., Marc, O., and Hovius, N.: Presentation and Analysis of a Worldwide Database of Earthquake-Induced Landslide Inventories, Journal of Geophysical Research: Earth Surface, 122, 2017JF004 236, https://doi.org/10.1002/2017JF004236, http://onlinelibrary.wiley.com/doi/10.1002/2017JF004236/abstract, 2017.

Uchida, T., Tamur, K., and Akiyama, K.: THE ROLE OF GRID CELL SIZE, FLOW ROUTING ALGOLITHM AND SPATIAL VARIABILITY OF SOIL DEPTH ON SHALLOW LANDSLIDE PREDICTION, in: 5th International Conference on Debris-Flow Hazards Mitigation: Mechanics, Prediction and Assessment, pp. 149–157, ITALIAN JOURNAL OF ENGINEERING GEOLOGY AND ENVIRONMENT, Padua, Italy, 2011.

Uchida, T., Sato, T., Mizuno, M., and Okamoto, A.: The role of rainfall magnitude on landslide characteristics triggered by Typhoon Tales, 2011 Civil engineering journal : 54(10), 10-13, 2012, Civil Engineering Journal (in Japanese), 54, 10–13, 2012.

Uchida, T., Okamoto, A., Kanbara, J. I., and Kuramoto, K.: RAINFALL THRESHOLDS FOR DEEP-SEATED RAPID LANDSLIDES, in: International Conference on Vajont 1963-2013 / Proceedings - Thoughts and analyses after 50 years since the catastrophic landslide, pp. 211–217, ITALIAN JOURNAL OF ENGINEERING GEOLOGY AND ENVIRONMENT, Padua, Italy, 2013.

Ushio, T., Sasashige, K., Kubota, T., Shige, S., Okamoto, K., Aonashi, K., Inoue, T., Takahashi, N., Iguchi, T., Kachi, M., Oki, R., Morimoto, T., and Kawasaki, Z.-I.: A Kalman Filter Approach to the Global Satellite Mapping of Precipitation (GSMaP) from Combined Passive Microwave and Infrared Radiometric Data, Journal of the Meteorological Society of Japan. Ser. II, 87A, 137–151, https://doi.org/10.2151/jmsj.87A.137, https://www.jstage.jst.go.jp/article/jmsj/87A/0/87A_0_137/_article, 2009.

Van Asch, T. W. J., Buma, J., and Van Beek, L. P. H.: A view on some hydrological triggering systems in landslides, Geomorphology, 30, 25–32, https://doi.org/10.1016/S0169-555X(99)00042-2, http://www.sciencedirect.com/science/article/pii/S0169555X99000422, 1999.

von Ruette, J., Lehmann, P., and Or, D.: Rainfall-triggered shallow landslides at catchment scale: Threshold mechanics-based modeling for abruptness and localization, Water Resources Research, 49, 6266–6285, https://doi.org/10.1002/wrcr.20418, https://agupubs.onlinelibrary.wiley.com/doi/abs/10.1002/wrcr.20418, 2013.

Wilson, R. C. and Wieczorek, G. F.: Rainfall Thresholds for the Initiation of Debris Flows at La Honda, California, Environmental & Engineering Geoscience, I, 11–27, https://doi.org/10.2113/gseegeosci.I.1.11, http://eeg.geoscienceworld.org/content/I/1/11, 1995.

Yagi, H., Sato, G., Higaki, D., Yamamoto, M., and Yamasaki, T.: Distribution and characteristics of landslides induced by the Iwate–Miyagi Nairiku Earthquake in 2008 in Tohoku District, Northeast Japan, Landslides, 6, 335–344, 2009.